



US008450014B2

(12) **United States Patent**  
**Liu et al.**

(10) **Patent No.:** **US 8,450,014 B2**  
(45) **Date of Patent:** **May 28, 2013**

(54) **LITHIUM ION BATTERIES WITH  
TITANIA/GRAPHENE ANODES**

(75) Inventors: **Jun Liu**, Richland, WA (US); **Daiwon Choi**, Richland, WA (US); **Zhenguo Yang**, Richland, WA (US); **Donghai Wang**, State College, PA (US); **Gordon L Graff**, West Richland, WA (US); **Zimin Nie**, Richland, WA (US); **Vilayanur V Viswanathan**, Richland, WA (US); **Jason Zhang**, Richland, WA (US); **Wu Xu**, Richland, WA (US); **Jin Yong Kim**, Richland, WA (US)

(73) Assignee: **Battelle Memorial Institute**, Richland, WA (US)

(\*) Notice: Subject to any disclaimer, the term of this patent is extended or adjusted under 35 U.S.C. 154(b) by 359 days.

(21) Appl. No.: **12/901,526**

(22) Filed: **Oct. 9, 2010**

(65) **Prior Publication Data**

US 2011/0111299 A1 May 12, 2011

**Related U.S. Application Data**

(63) Continuation-in-part of application No. 12/460,993, filed on Jul. 27, 2009, now Pat. No. 8,257,867.

(60) Provisional application No. 61/084,140, filed on Jul. 28, 2008.

(51) **Int. Cl.**

<b>H01M 4/13</b>	(2010.01)
<b>H01M 4/58</b>	(2010.01)
<b>H01M 6/00</b>	(2006.01)
<b>H01M 10/00</b>	(2006.01)
<b>H01M 4/02</b>	(2006.01)
<b>H01G 4/28</b>	(2006.01)
<b>C01B 31/04</b>	(2006.01)
<b>C01B 31/00</b>	(2006.01)

**B23P 17/04** (2006.01)

**H01S 4/00** (2006.01)

(52) **U.S. Cl.**

USPC ..... **429/231.5**; 29/592; 29/592.1; 423/448;  
423/445  
R; 423/414; 429/122; 429/209; 361/306.3

(58) **Field of Classification Search**

USPC ..... 29/592, 592.1; 423/448, 445 R, 414;  
429/122, 209, 231.5; 361/306.3  
See application file for complete search history.

(56) **References Cited**

**U.S. PATENT DOCUMENTS**

5,972,088 A	10/1999	Krishnan et al.
6,492,014 B1	12/2002	Rolison et al.

(Continued)

**FOREIGN PATENT DOCUMENTS**

CN	1483212	3/2004
CN	1588679	3/2005

(Continued)

**OTHER PUBLICATIONS**

Slack (Journal of Applied Physics 1964 vol. 35 pp. 3460-3466).\*

(Continued)

*Primary Examiner* — Patrick Ryan

*Assistant Examiner* — Aaron Greso

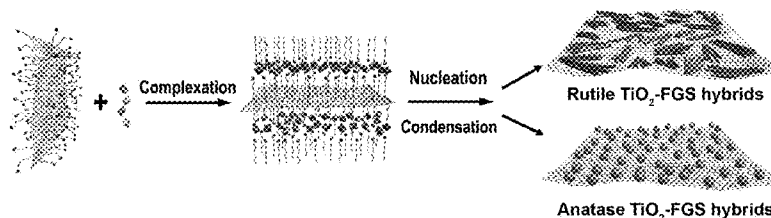
(74) *Attorney, Agent, or Firm* — Klarquist Sparkman, LLP

(57)

**ABSTRACT**

Lithium ion batteries having an anode comprising at least one graphene layer in electrical communication with titania to form a nanocomposite material, a cathode comprising a lithium olivine structure, and an electrolyte. The graphene layer has a carbon to oxygen ratio of between 15 to 1 and 500 to 1 and a surface area of between 400 and 2630 m<sup>2</sup>/g. The nanocomposite material has a specific capacity at least twice that of a titania material without graphene material at a charge/discharge rate greater than about 10 C. The olivine structure of the cathode of the lithium ion battery of the present invention is LiMPO<sub>4</sub> where M is selected from the group consisting of Fe, Mn, Co, Ni and combinations thereof.

**8 Claims, 15 Drawing Sheets**



## U.S. PATENT DOCUMENTS

7,094,499	B1	8/2006	Hung	
7,623,340	B1	11/2009	Song et al.	
8,257,867	B2	9/2012	Liu et al.	
2002/0022122	A1	2/2002	Hirata et al.	
2002/0054995	A1	5/2002	Mazurkiewicz	
2002/0192137	A1 *	12/2002	Chaloner-Gill et al.	..... 423/306
2003/0086859	A1	5/2003	Kawakami et al.	
2004/0120880	A1	6/2004	Zhang et al.	
2004/0131934	A1	7/2004	Sugnaux et al.	
2004/0137225	A1	7/2004	Balkus, Jr. et al.	
2004/0150140	A1	8/2004	Zhan et al.	
2006/0154071	A1	7/2006	Homma et al.	
2007/0092432	A1	4/2007	Prud'homme et al.	
2007/0158618	A1	7/2007	Song et al.	
2007/0212538	A1	9/2007	Niu	
2007/0281854	A1	12/2007	Harbour et al.	
2008/0063585	A1	3/2008	Smalley et al.	
2008/0258359	A1	10/2008	Zhamu et al.	
2008/0279756	A1	11/2008	Zhamu et al.	
2008/0312368	A1	12/2008	Prud'homme et al.	
2009/0117467	A1 *	5/2009	Zhamu et al.	..... 429/231.8
2009/0246625	A1	10/2009	Lu	
2009/0290897	A1	11/2009	Doshoda et al.	
2009/0297947	A1	12/2009	Deng et al.	
2009/0303660	A1	12/2009	Nair et al.	
2009/0305135	A1	12/2009	Shi et al.	
2010/0081057	A1	4/2010	Liu et al.	
2010/0143798	A1	6/2010	Zhamu et al.	
2010/0159366	A1	6/2010	Shao-Horn et al.	
2011/0033746	A1	2/2011	Liu et al.	
2011/0045347	A1	2/2011	Liu et al.	
2011/0051316	A1	3/2011	Liu et al.	
2012/0088158	A1	4/2012	Liu et al.	
2012/0295027	A1	11/2012	Liu et al.	
2012/0295096	A1	11/2012	Liu et al.	
2012/0305165	A1	12/2012	Liu et al.	

## FOREIGN PATENT DOCUMENTS

CN	1793451	6/2006
CN	101048055	10/2007
CN	101139090	3/2008
JP	10233211	9/1998
WO	WO2007/015710	2/2007
WO	WO 2007/061945	* 5/2007
WO	WO2007/061945	5/2007
WO	WO2008/106991	9/2008
WO	WO2009/023051	2/2009
WO	WO 2009/085015	* 7/2009
WO	WO2010/014215	2/2010
WO	WO2010/030361	3/2010
WO	WO2011/019764	2/2011
WO	WO2011/019765	2/2011

## OTHER PUBLICATIONS

Mockenstun (ADMASM Proceedings of the ASME App Mech Div 2005; taken as November pp. 277-291).\*

Choi et al., "Li-ion batteries from LiFePO<sub>4</sub> cathode and anatase/graphene composite anode for stationary energy storage," *Electrochemistry Communications* 12(3):378-381 (Jan. 2010).

Franger et al., "Optimized Lithium Iron Phosphate for High-Rate Electrochemical Application," *Journal of the Electrochemical Society*, vol. 151, No. 7, pp. A1024-A1027 (May 2004).

International Search Report and Written Opinion for PCT/US2011/047144 (mailed Feb. 23, 2012).

International Search Report and Written Opinion for PCT/US2011/055216 (mailed Apr. 23, 2012).

International Search Report and Written Opinion for PCT/US2011/62016 (mailed Apr. 9, 2012).

Bizdoaca et al., "Magnetically directed self-assembly of submicron spheres with a Fe<sub>3</sub>O<sub>4</sub> nanoparticle shell," *Journal of Magnetism and Magnetic Materials*, 240(1-3):44-46 (Feb. 2002).

Gómez-Navarro et al., "Electronic Transport Properties of Individual Chemically Reduced Graphene Oxide Sheets," *Nano Letters*, 7(11):3499-3503 (Oct. 2007).

Lindsay, "Data analysis and anode materials for lithium ion batteries," PhD Thesis, University of Wollongong Thesis Collection, Ch. 2, Section 2.5.5, <http://ro.uow.edu.au/theses/359> (2004).

Office action from U.S. Patent and Trademark Office for U.S. Appl. No. 12/460,993, mailed Jan. 19, 2012.

Office action from U.S. Patent and Trademark Office for U.S. Appl. No. 12/462,857, mailed Jan. 10, 2012.

Office action from U.S. Patent and Trademark Office for U.S. Appl. No. 12/852,794, mailed Jan. 23, 2012.

Ribeiro et al., "Assembly and Properties of Nanoparticles," *Nanostructure Science and Technology*, 33-79, see 62-63, 77 (2009).

Superior Graphite Company, "Development of Low cost Carbonaceous Materials for Anodes in Lithium-Ion Batteries for Electric and Hybrid Electric Vehicles," DE-F02-00EE50630, 50 pages (Dec. 10, 2002).

Tung et al., "Low-temperature solution processing of graphene-carbon nanotube hybrid materials for high-performance transparent conductors," *Nano Lett.*, 9(5):1949-1955 (Apr. 2009).

U.S. Appl. No. 12/980,328, filed Dec. 28, 2010.

Wang et al., "Microemulsion Syntheses of Sn and SnO<sub>2</sub>-Graphite Nanocomposite Anodes for Li-Ion Batteries," *Journal of the Electrochemical Society*, 151(4):A563-A570 (Feb. 20, 2004).

Wang et al., "Self-Assembled TiO<sub>2</sub>-Graphene Hybrid Nanostructures for Enhanced Li-Ion Insertion," *ACS Nano*, 3(4):907-914 (Mar. 26, 2009).

Wang, et al., "Synthesis and Li-Ion Insertion Properties of Highly Crystalline Mesoporous Rutile TiO<sub>2</sub>," *Chem. Mater.*, 20:3435-3442 (May 2008).

Wang et al., "Tin Nanoparticle Loaded Graphite Anodes for Li-Ion Battery Applications," *Journal of the Electrochemical Society*, 151(11):A563-A570 (Oct. 4, 2004).

Xu et al., "Assembly of chemically modified graphene: methods and applications," *J. Mater. Chem.*, 21:3311-3323 (Mar. 2011).

Aksay et al., "Biomimetic Pathways for Assembling Inorganic Thin Films," *Science* 273:892-898 (Aug. 1996).

Aricò et al., "Nanostructured materials for advanced energy conversion and storage devices," *Nature Materials* 4:366-377 (May 2005).

Armstrong et al., "TiO<sub>2</sub>-B Nanowires," *Angewandte Chemie-International Edition* 43:2286-2288 (Apr. 2004).

Armstrong et al., "TiO<sub>2</sub>(B) Nanowires as an Improved Anode Material for Lithium-Ion Batteries Containing LiFePO<sub>4</sub> or LiNi<sub>0.5</sub>Mn<sub>1.5</sub>O<sub>4</sub> Cathodes and a Polymer Electrolyte," *Advanced Materials* 18:2597-2600 (Oct. 2006).

Asefa et al., "Periodic mesoporous organosilicas with organic groups inside the channel walls," *Nature* 402:867-871 (Dec. 1999).

Atkin et al., "Self-Assembly of a Nonionic Surfactant at the Graphite/Ionic Liquid Interface," *Journal of the American Chemical Society* 127:11940-11941 (Aug. 2005).

Attard et al., "Mesoporous Platinum Films from Lyotropic Liquid Crystalline Phases," *Science* 278:838-840 (Oct. 1997).

Bagshaw et al., "Templating of Mesoporous Molecular Sieves by Nonionic Polyethylene Oxide Surfactants," *Science* 269:1242-1244 (Sep. 1995).

Baudrin et al., "Structural evolution during the reaction of Li with nano-sized rutile type TiO<sub>2</sub> at room temperature," *Electrochemistry Communications* 9:337-342 (Feb. 2007).

Berger et al., "Electronic Confinement and Coherence in Patterned Epitaxial Graphene," *Science* 312:1191-1196 (May 2006).

Bonard et al., "Purification and Size-Selection of Carbon Nanotubes," *Advanced Materials* 9(10):827-831 (month unknown 1997).

Braun et al., "Semiconducting superlattices template by molecular assemblies," *Nature* 380:325-328 (Mar. 1996).

Chen et al., "Mechanically Strong, Electrically Conductive, and Biocompatible Graphene Paper," *Advanced Materials* 20:3557-3561 (Jul. 2008).

Chen et al., "Reducing Carbon in LiFePO<sub>4</sub>/C Composite Electrodes to Maximize Specific Energy, Volumetric Energy, and Tap Density," *Journal of the Electrochemical Society* 149(9):A1184-A1189 (Sep. 2002).

Decher, "Fuzzy Nanoassemblies: Toward Layered Polymeric Multicomposites," *Science* 277(9):1232-1237 (Aug. 1997).

- Dikin et al., "Preparation and characterization of graphene oxide paper," *Nature* 448:457-460 (Jul. 2007).
- Dominko et al., "Impact of the Carbon Coating Thickness on the Electrochemical Performance of LiFePO<sub>4</sub>/C Composites," *Journal of the Electrochemical Society* 152(3):A607-A610 (Jan. 2005).
- Erjavec et al., "RuO<sub>2</sub>-wired high-rate nanoparticulate TiO<sub>2</sub> (anatase): Suppression of particle growth using silica," *Electrochemistry Communications* 10:926-929 (Jun. 2008).
- Gómez-Navarro et al., "Electronic Transport Properties of Individual Chemically Reduced Graphene Oxide Sheets," *American Chemical Society* 7(11):3499-3503 (Oct. 2007).
- Goward et al., "Poly(pyrrole) and poly(thiophene)/vanadium oxide interleaved nanocomposites: positive electrodes for lithium batteries," *Electrochimica Acta* 43(10-11):1307-1303 (Apr. 1998).
- Guo et al., "Superior Electrode Performance of Nanostructured Mesoporous TiO<sub>2</sub> (Anatase) through Efficient Hierarchical Mixed Conducting Networks," *Advanced Materials* 19:2087-2091 (Jul. 2007).
- Herle et al., "Nano-network electronic conduction in iron and nickel olivine phosphates," *Nature Materials* 3:147-152 (Feb. 2004).
- Hu et al., "High Lithium Electroactivity of Nanometer-Sized Rutile TiO<sub>2</sub>," *Advanced Materials* 18:1421-1426 (Apr. 2006).
- Hu et al., "Improved Electrode Performance of Porous LiFePO<sub>4</sub> Using RuO<sub>2</sub> as an Oxidic Nanoscale Interconnect," *Advanced Materials* 19:1963-1966 (Jul. 2007).
- Huang et al., "Self-organizing high-density single-walled carbon nanotube arrays from surfactant suspensions," *Nanotechnology* 15:1450-1454 (Nov. 2004).
- Huo et al., "Organization of Organic Molecules with Inorganic Molecular Species into Nanocomposite Biphase Arrays," *Chemistry Materials* 6:1176-1191 (Aug. 1994).
- International Preliminary Report on Patentability and Written Opinion for PCT/US2009/005085, mailed Mar. 24, 2011.
- International Search Report and Written Opinion for PCT/US2009/004369, mailed Jan. 29, 2010.
- International Search Report for PCT/US2009/005085, mailed Feb. 4, 2010.
- International Search Report for PCT/US2010/045088, mailed Oct. 6, 2010.
- International Search Report for PCT/US2010/045089, mailed Oct. 27, 2010.
- Jiang et al., "Nanocrystalline Rutile TiO<sub>2</sub> Electrode for High-Capacity and High-Rate Lithium Storage," *Electrochemical and Solid-State Letters* 10(5):A127-A129 (Mar. 2007).
- Kavan et al., "Nanocrystalline TiO<sub>2</sub> (Anatase) Electrodes: Surface Morphology, Adsorption, and Electrochemical Properties," *Journal of the Electrochemical Society* 143(2):394-400 (Feb. 1996).
- Kresge et al., "Ordered mesoporous molecular sieves synthesized by a liquid-crystal template mechanism," *Nature* 359:710-712 (Oct. 1992).
- Leroux et al., "Electrochemical Lithium Intercalation into a Polyaniline/V<sub>2</sub>O<sub>5</sub> Nanocomposite," *J. Electrochemical Society* 143(9):L181-L183 (Sep. 1996).
- Li et al., "Processable aqueous dispersions of graphene nanosheets," *Nature Nanotechnology* 3:101-105 (Jan. 2008).
- Liu et al., "Oriented Nanostructures for Energy Conversion and Storage," *ChemSusChem* 1:676-697 (Aug. 2008).
- Lou et al., "Template-Free Synthesis of SnO<sub>2</sub> Hollow Nanostructures with High Lithium Storage Capacity," *Advanced Materials* 18:2325-2329 (Aug. 2006).
- Maier et al., "Nanoionics: ion transport and electrochemical storage in confined systems," *Nature Materials* 4:805-815 (Nov. 2005).
- Mao et al., "Structural, electronic and magnetic properties of manganese doping in the upper layer of bilayer graphene," *Nanotechnology* 19(20):205708-205715 (May 2008).
- McAllister et al., "Single Sheet Functionalized Graphene by Oxidation and Thermal Expansion of Graphite," *Chemical Materials* 19:4396-4404 (May 2007).
- Moriguchi et al., "A Mesoporous Nanocomposite of TiO<sub>2</sub> and Carbon Nanotubes as a High-Rate Li-Intercalation Electrode Material," *Advanced Materials* 18:69-73 (Jan. 2006).
- Moskon et al., "Citrate-Derived Carbon Nanocoatings for Poorly Conducting Cathode," *Journal of the Electrochemical Society* 153(10):A1805-A1811 (Jul. 2006).
- Nethravathi, et al., "Graphite Oxide-Intercalated Anionic Clay and Its Decomposition to Graphene-Inorganic Material Nanocomposites," *Langmuir* 24:8240-8244 (Aug. 2008).
- Nishihara et al., "Carbon-coated mesoporous silica with hydrophobicity and electrical conductivity," *Carbon* 46(1):pp. 48-53 (Jan. 2008).
- Niyogi et al., "Solution Properties of Graphite and Graphene," *Journal of the American Chemical Society* 128:7720-7721 (Jan. 2006).
- Novoselov et al., "Electric Field Effect in Atomically Thin Carbon Films," *Science* 306:666-669 (Oct. 2004).
- Office action from U.S. Patent and Trademark Office for U.S. Appl. No. 12/553,527, mailed Nov. 10, 2011.
- Paek et al., "Enhanced Cyclic Performance and Lithium Storage Capacity of SnO<sub>2</sub>/Graphene Nanoporous Electrodes with Three-Dimensionally Delaminated Flexible Structure," *Nano Letters* 9(1):72-75 (Dec. 2008).
- Peigney et al., "Specific surface area of carbon nanotubes and bundles of carbon nanotubes," *Carbon* 39:507-514 (Apr. 2001).
- Prossini et al., "Improved electrochemical performance of a LiFePO<sub>4</sub>-based composite cathode," *Electrochimica Acta* 46:3517-3523 (Aug. 2001).
- Ramanathan et al., "Functionalized graphene sheets for polymer nanocomposites," *Nature Nanotechnology* 3:327-331 (May 2008).
- Read et al., z"SnO<sub>2</sub>-carbon composites for lithium-ion battery anodes," *Journal of Power Sources* 96:277-281 (Jun. 2001).
- Reddy et al., "Room temperature synthesis and Li insertion into nanocrystalline rutile TiO<sub>2</sub>," *Electrochemistry Communications* 8:1299-1303 (Aug. 2006).
- Restriction Requirement from the U.S. Patent and Trademark Office for U.S. Appl. No. 12/462,857, mailed Aug. 22, 2011.
- Restriction Requirement from the U.S. Patent and Trademark Office for U.S. Appl. No. 12/553,527, mailed Sep. 26, 2011.
- Richard et al., "Supramolecular Self-Assembly of Lipid Derivatives on Carbon Nanotubes," *Science* 300:775-778 (May 2003).
- Sakamoto et al., "Hierarchical battery electrodes based on inverted opal structures," *Journal of Materials Communication* 12:2859-2861 (Aug. 2002).
- Schniepp et al., "Functionalized Single Graphene Sheets Derived from Splitting Graphite Oxide," *The Journal of Physical Chemistry Letters* 110:8535-8539 (Apr. 2006).
- Schniepp et al., "Self-Healing of Surfactant Surface Micelles on Millisecond Time Scales," *Journal of the American Chemical Society* 128:12378-12379 (Aug. 2006).
- Si, et al., "Synthesis of Water Soluble Graphene," *Nano Letters* 8(6):1679-1682 (May 2008).
- Srinivas, et al., "Molecular Dynamics Simulations of Surfactant Self-Organization at a Solid-Liquid Interface," *Journal of the American Chemical Society* 128(3):848-853 (Jan. 2006).
- Stankovich et al., "Graphene-based composite materials," *Nature* 442:282-286 (Jul. 2006).
- Stankovich et al., "Stable aqueous dispersions of graphitic nanoplatelets via the reduction of exfoliated graphite oxide in the presence of poly(sodium 4-styrenesulfonate)," *Journal of Materials Chemistry* 16:155-158 (document marked Nov. 2005).
- Stoller et al., "Graphene-Based Ultra capacitors," *Nano Letters* 8(10):3498-3502 (Sep. 2008).
- Suzuki et al., "H-T phase diagram and the nature of vortex-glass phase in a quasi-two-dimensional superconductor: Sn-metal layer sandwiched between graphene sheets," *Physica C: Superconductivity* 402(3):243-256 (Nov. 2003).

- Tanaka et al., "Characteristics of graphene-layer encapsulated nanoparticles fabricated using laser ablation method," *Diamond and Related Materials* 17(4-5):664-668 (Nov. 2007).
- Tarascon et al., "Issues and challenges facing rechargeable lithium batteries," *Nature* 414:359-367 (Nov. 2001).
- Wang, et al., "Surface-Mediated Growth of Transparent, Oriented, and Well-Defined Nanocrystalline Anatase Titania Films," *Journal of the American Chemical Society* 128:13670-13671 (Oct. 2006).
- Wang et al., "Low-Temperature Synthesis of Tunable Mesoporous Crystalline Transition Metal Oxides and Applications as Au Catalyst Supports," *Chemistry of Materials* 20:13499-13509 (Aug. 2008).
- Wang, et al., "Synthesis and Li-Ion Insertion Properties of Highly Crystalline Mesoporous Rutile TiO<sub>2</sub>," *American Chemical Society* 20:3435-3442 (May 2008).
- Wang, et al., "Atomic Layer Deposition of Metal Oxides on Pristine and Functionalized Graphene," *Journal of the American Chemical Society* 130:8152-8153 (Jun. 2008).
- Wang, et al., "Cooperative Self-Assembly of Tertiary Systems: Novel Graphene-Metal Oxide Nanocomposites," *Pacific Northwest National Laboratory and Princeton University* 21 pages (date unknown).
- Watcharotone et al., "Graphene-Silica Composite Thin Films as Transparent Conductors," *Nano Letters* 7(7):1888-1892 (Jun. 2007).
- Whitesides, et al., "Molecular Self-Assembly and Nanochemistry: A Chemical Strategy for the Synthesis of Nanostructures," *Science* 254:1312-1319 (Nov. 1991).
- Williams, et al., "TiO<sub>2</sub>-Graphene Nanocomposites. UV-Assisted Photocatalytic Reduction of Graphene Oxide," *Acs Nano* 2(7):1487-1491 (Jul. 2008).
- Xu, et al., "Flexible Graphene Films via the Filtration of Water-Soluble Noncovalent Functionalized Graphene Sheets," *Journal of the American Chemical Society* 130:5856-5857 (Apr. 2008).
- Yamabi, et al., "Crystal Phase Control for Titanium Dioxide Films by Direct Deposition in Aqueous Solutions," *Chemical Materials* 14:609-614 (Jan. 2002).
- Yang, et al., "Generalized syntheses of large-pore mesoporous metal oxides with semicrystalline frameworks," *Nature* 396:152-155 (Nov. 1998).
- Yoo, et al., "Large Reversible Li Storage of Graphene Nanosheet Families for Use in Rechargeable Lithium Ion Batteries," *Nano Letters* 8(8):2277-2282 (Aug. 2008).
- Zhao et al., "Triblock Copolymer Syntheses of Mesoporous Silica with Periodic 50 to 300 Angstrom Pores," *Science* 279:548-552 (Jan. 1998).
- Zhou et al., "Lithium Insertion into TiO<sub>2</sub> Nanotube Prepared by the Hydrothermal Process," *Journal of the Electrochemical Society* 150(9):A1246-A1249 (Jul. 2003).
- Zukalová et al., "Pseudocapacitive Lithium Storage in TiO<sub>2</sub>(B)," *Chemistry of Materials* 17:1248-1255 (Feb. 2005).
- Final Office action from U.S. Patent and Trademark Office for U.S. Appl. No. 12/462,857, mailed Aug. 23, 2012.
- Final Office action from U.S. Patent and Trademark Office for U.S. Appl. No. 12/553,527, mailed Nov. 20, 2012.
- Final Office action from U.S. Patent and Trademark Office for U.S. Appl. No. 12/852,794, mailed Jul. 3, 2012.
- International Preliminary Report on Patentability and Written Opinion for PCT/US2009/004369 (mailed Feb. 10, 2011).
- International Preliminary Report on Patentability and Written Opinion for PCT/US2010/045088 (mailed Feb. 23, 2012).
- International Preliminary Report on Patentability and Written Opinion for PCT/US2010/045089 (mailed Feb. 23, 2012).
- Kang et al., "The Cycling Performance of Graphite Electrode Coated with Tin Oxide for Lithium Ion Battery," *Journal of the Korean Electrochemical Society*, 5(2):52-56 (May 2002).
- Lee, "Dispersion of Sn and SnO on carbon anodes," *Journal of Power Sources*, 90(1):70-75 (Sep. 2000).
- McDermott et al., "Electron Transfer Kinetics of Aqueated Fe<sup>+3/+2</sup>, Eu<sup>+3/+2</sup>, and V<sup>+3/+2</sup> at Carbon Electrodes," *Journal of the Electrochemical Society*, 140(9):2593-2599 (Sep. 1993).
- Mdleleni et al., "Sonochemical Synthesis of Nanostructured Molybdenum Sulfide," *Journal of the American Chemical Society*, 12:6189-6190 (Jun. 1998).
- Mockensturm et al., "Van Der Waals' Elastica," *2005 ASME International Mechanical Engineering Congress and Exposition*, 277-291 (Nov. 5-11, 2005).
- Murakami et al., "Formation of Positronium in Cup-stacked Carbon Nanofibers," (Abstract and Introduction Only) *Materials Science Forum*, 445-446:331-333 (Jan. 2004).
- Nakahara et al., "Structural changes of a pyrolytic graphite surface oxidized by electrochemical and plasma treatment," *Journal of Materials Science*, 29(12):3193-3199 (Jun. 1994).
- Notice of Allowance from U.S. Patent and Trademark Office for U.S. Appl. No. 12/460,993, mailed Jul. 11, 2012.
- Office action from the Chinese Patent Office for Chinese Patent Application No. 200980135205.8, mailed Nov. 14, 2012.
- Office action from the Chinese Patent Office for Chinese Patent Application No. 200980129673.4, mailed Sep. 10, 2012.
- Office action from U.S. Patent and Trademark Office for U.S. Appl. No. 12/553,527, mailed Jun. 1, 2012.
- Office action from U.S. Patent and Trademark Office for U.S. Appl. No. 12/980,328, mailed Feb. 27, 2013.
- Office action from U.S. Patent and Trademark Office for U.S. Appl. No. 13/559,528, mailed Jan. 10, 2013.
- Office action from U.S. Patent and Trademark Office for U.S. Appl. No. 13/585,741, mailed Jan. 14, 2013.
- Ou et al., "Characteristics of graphene-layer encapsulated nanoparticles fabricated using laser ablation method," *Diamond and Related Materials*, 17(4-5):664-668 (Apr.-May 2008).
- Restriction Requirement from the U.S. Patent and Trademark Office for U.S. Appl. No. 12/901,527, mailed Dec. 13, 2012.
- Shao, "Influencing Surface Tension," *California State Science Fair 2006 Project Summary* Project No. J0531 <http://www.usc.edu/CSSF/History/2006/Projects/J0531.pdf> (Apr. 2006).
- Suslick et al., "Sonochemical synthesis of amorphous iron," *Nature*, 353:414-416 (Oct. 1991).
- USP, "Material Safety Data Sheet—Sodium Lauryl Sulfate," Catalog No. 1614363 (Oct. 28, 2010).
- Wakihara et al., "Lithium Ion Batteries Fundamentals and Performance," Wiley-VCH, New York (1998).
- Walker, *Just the Facts 101 Textbook Key Facts, Physics*, vol. 1, Chapter 15 Fluids, p. 13 <http://books.google.com/books?id=fhRX6IFg2fcC&pg=PT278lpg=PT278&dq=%22Surfactants+are+compounds+that+lower+the+surface+tension+of+a+liquid%22+-2012+-2011+-2010+-2009&source=bl&ots=cVS1AJ-GOS&sig=e9wgCJkhGYTe2zdqoql1y-iQG1o&hl=en&sa=X&ei=-6ErUO6NO6Wo0AGh74D4Bw&ved=OCEUQ6AEwBA#v=onepage&q=%22Surfactants%20are%20compounds%20that%20lower%20the%20surface%20tension%20of%20a%20liquid%22%20-20-2012%20-2011%20-2010%20-2009&f=false>.
- Yao et al., "In situ chemical synthesis of SnO<sub>2</sub>-graphene nanocomposite as anode materials for lithium-ion batteries," *Electrochemistry Communications*, 11:1849-1852 (Aug. 2009).
- Yu et al., "Mesoporous tin oxides as lithium intercalation anode materials," *Journal of Power Sources*, 104:97-100 (Jan. 2002).

Fig. 1

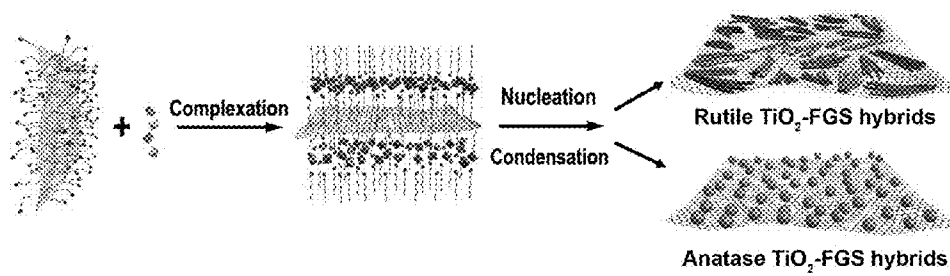


Fig.2

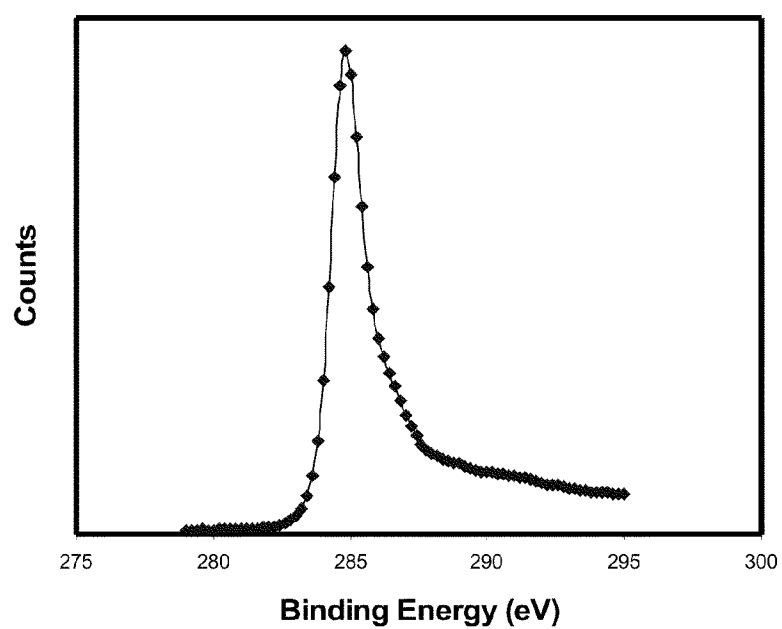


Fig.3

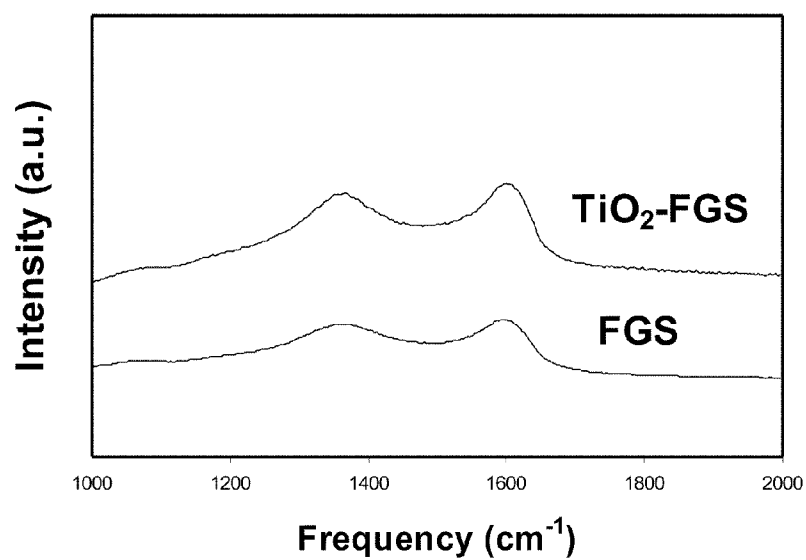


Fig. 4

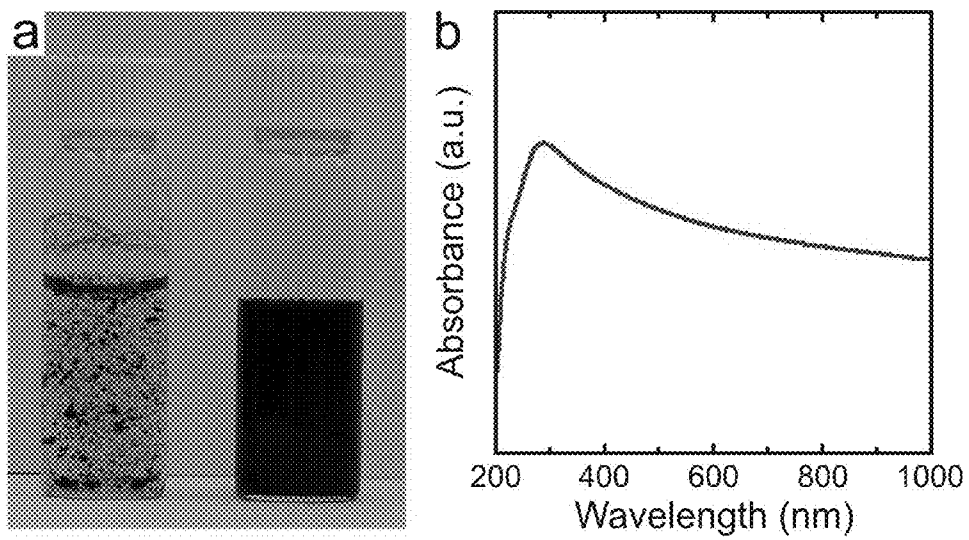




Fig.5

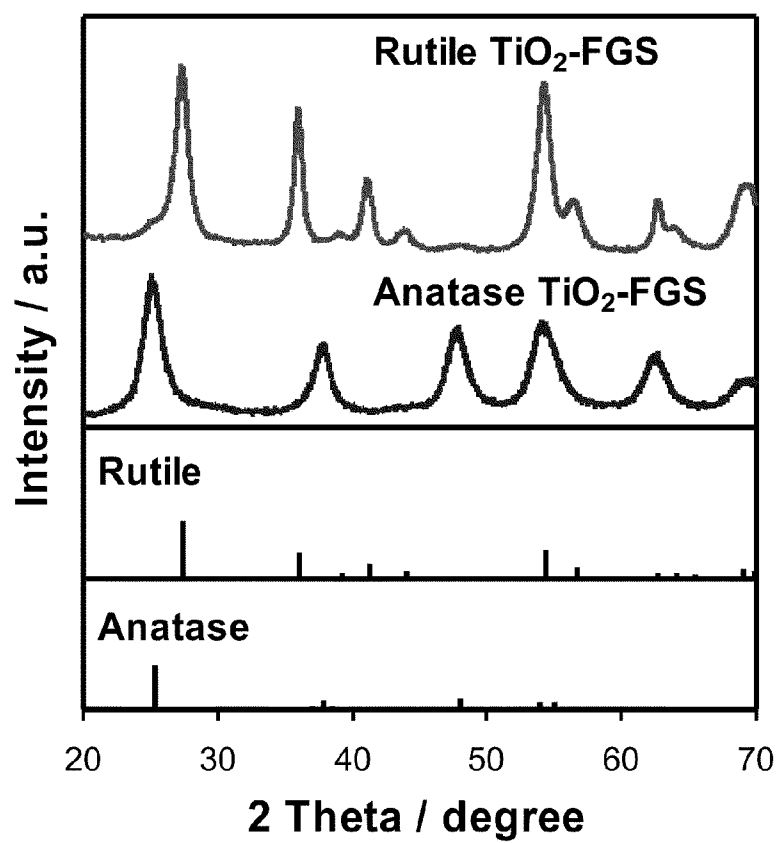


Fig.6

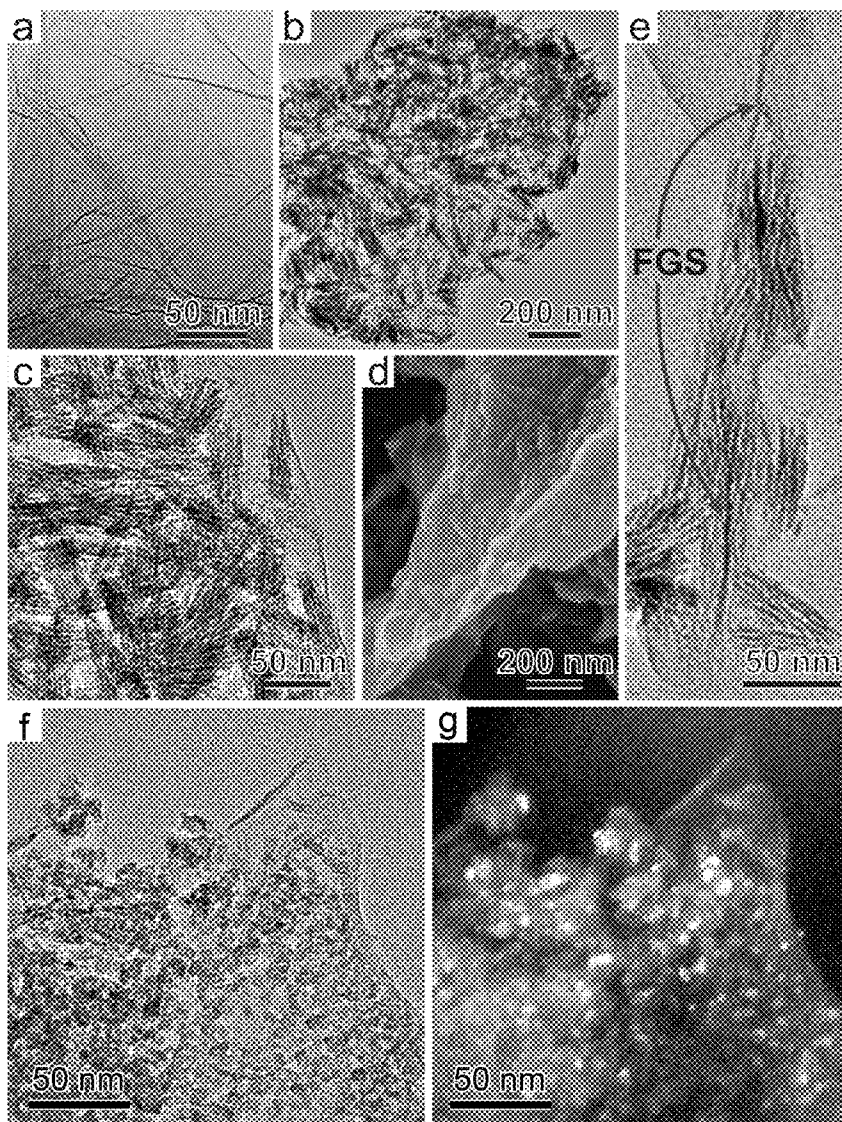


Fig. 7

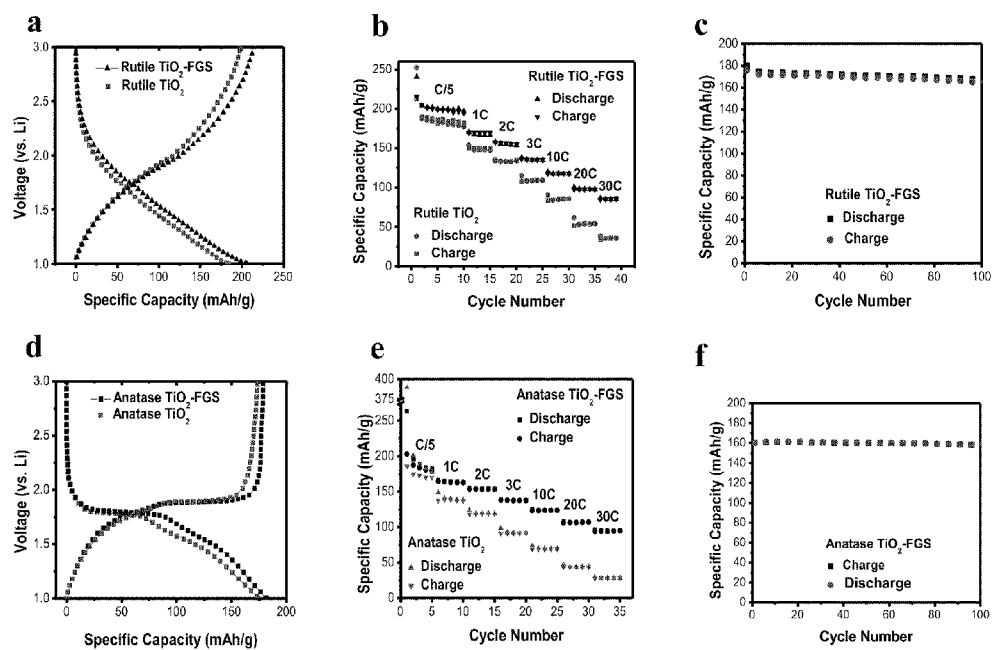


Fig.8

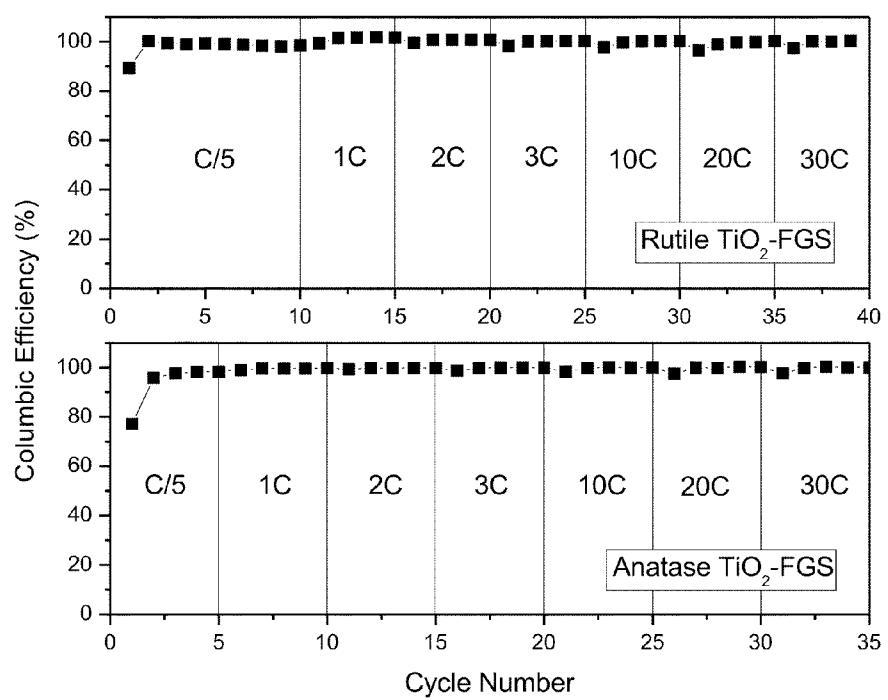


Fig.9

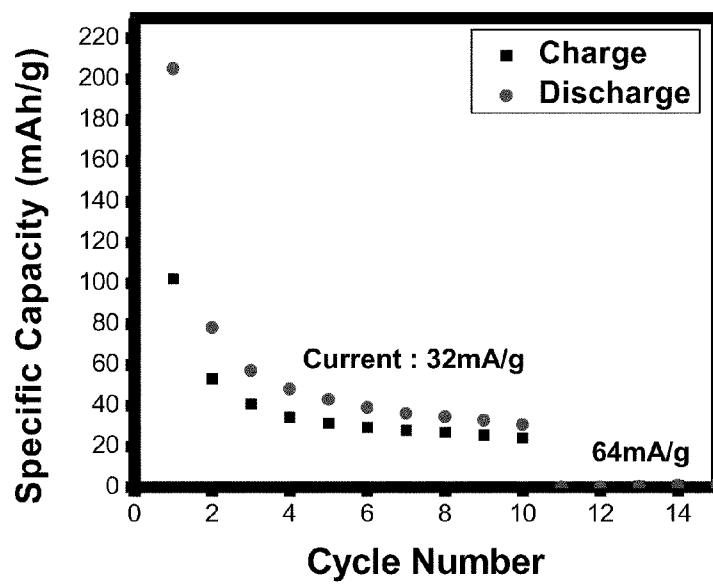


Fig.10

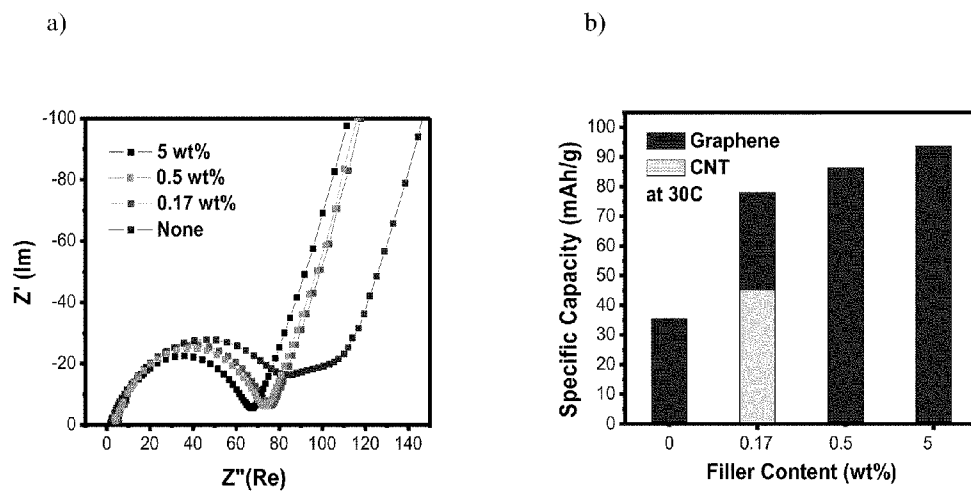


Fig.11

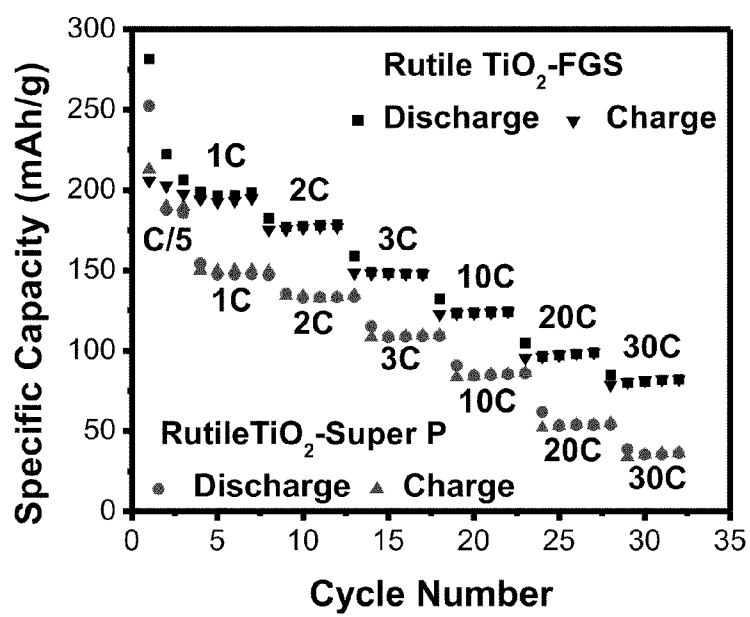
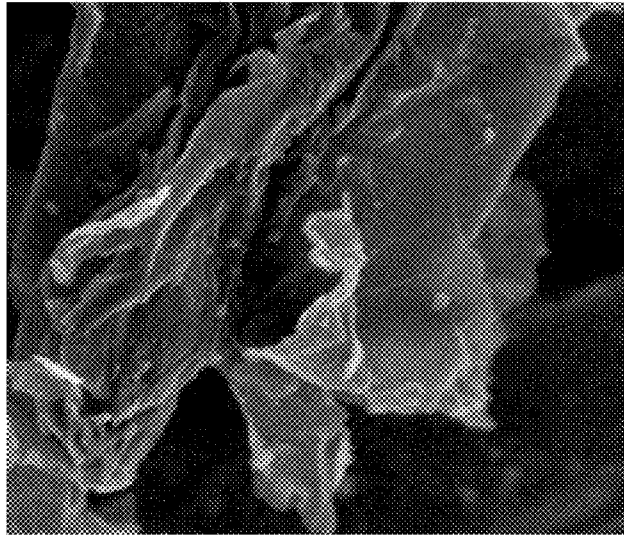
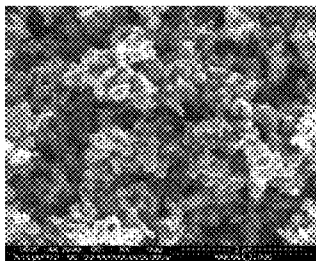


Fig. 12





(a)



(b)

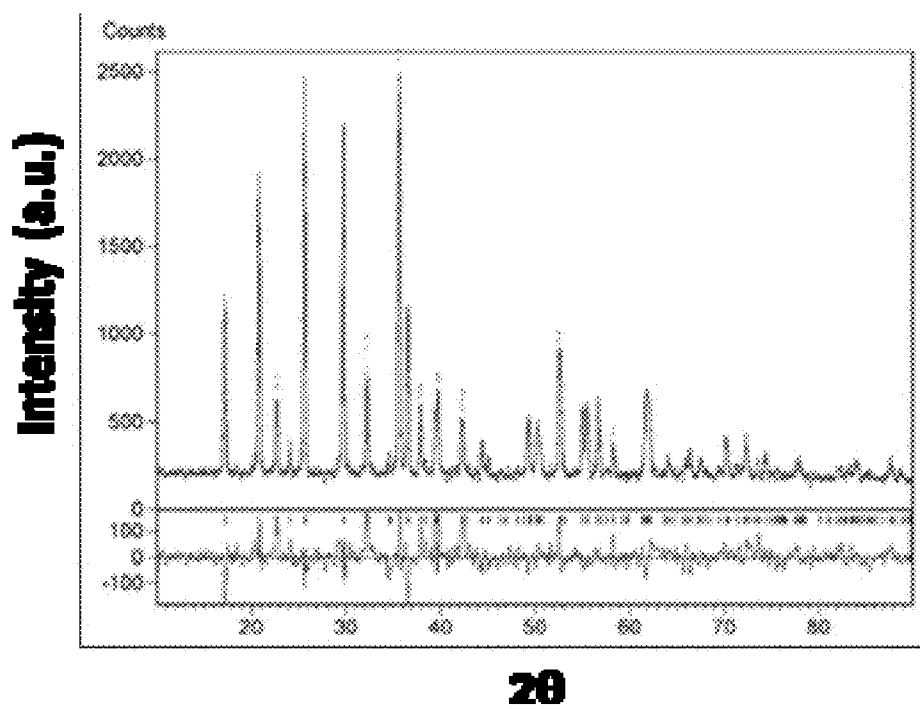
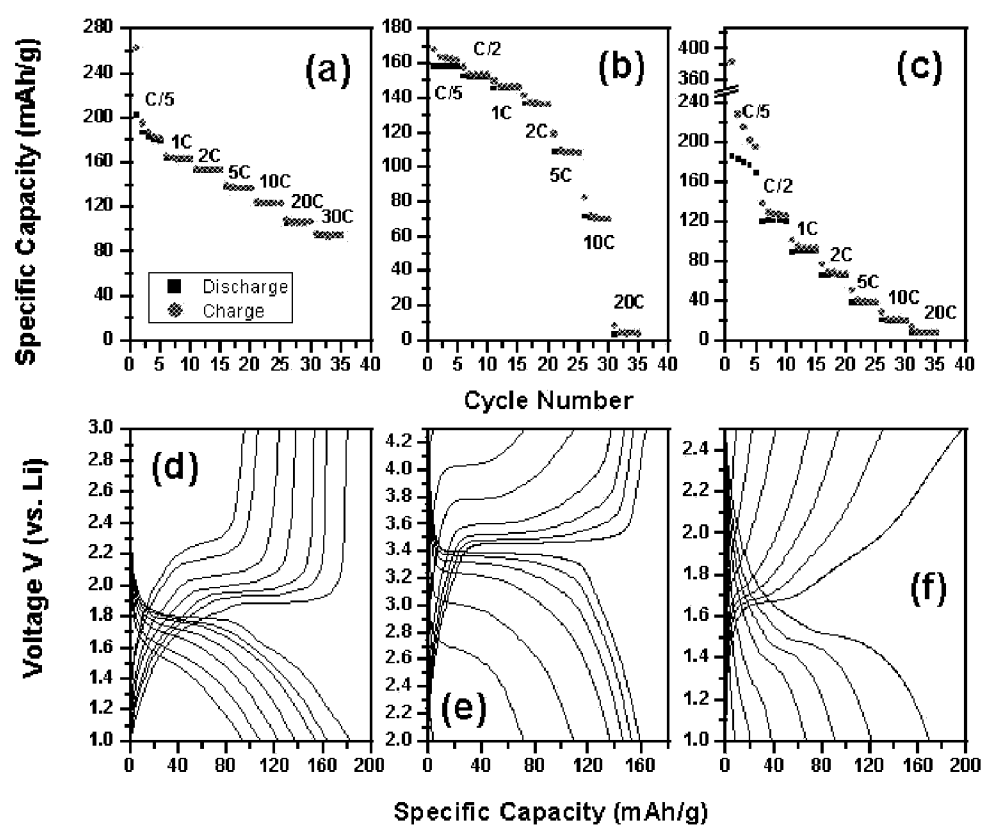
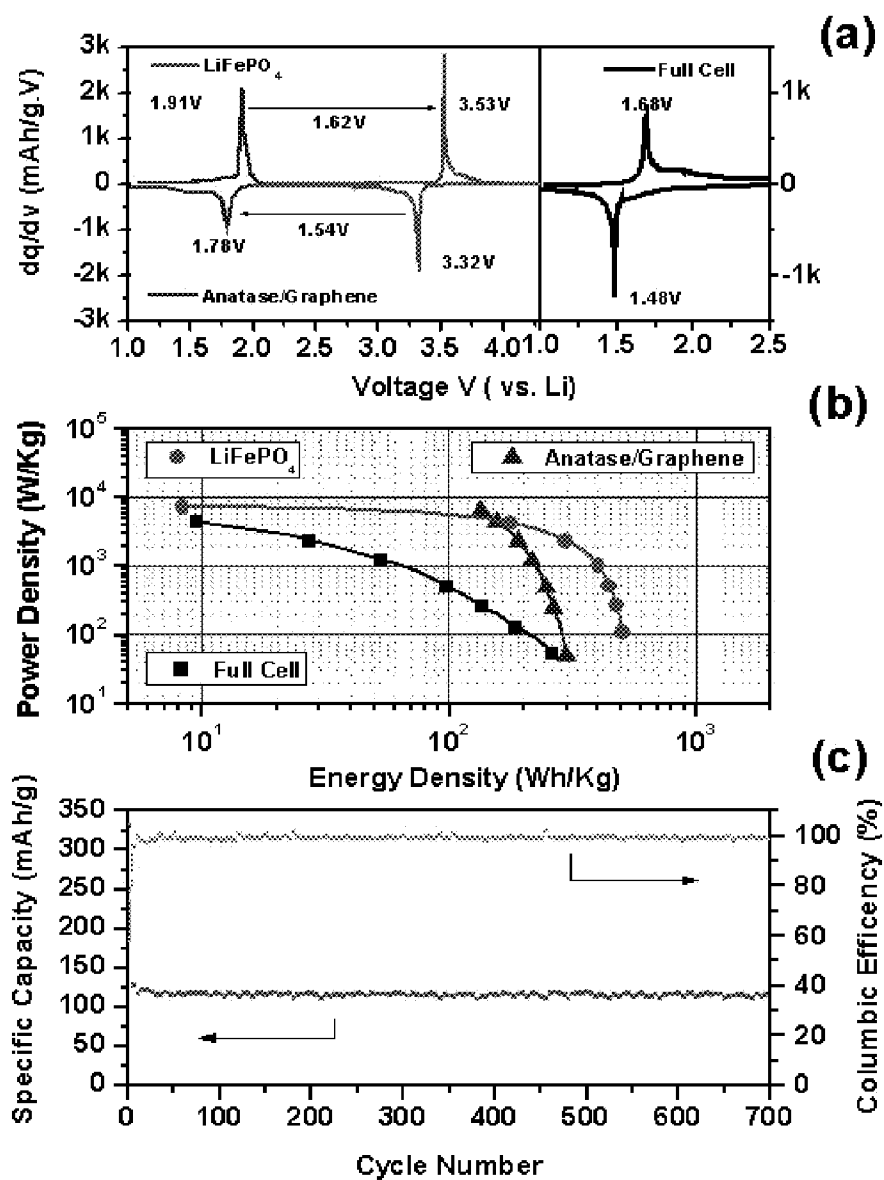


Figure 13

Figure 14





1

# LITHIUM ION BATTERIES WITH TITANIA/GRAPHENE ANODES

## CROSS REFERENCE TO RELATED APPLICATIONS

This application is a continuation in part of U.S. Ser. No. 12/460,993 filed Jul. 27, 2009, now U.S. Pat. No. 8,257,867 which claims priority to U.S. Provisional Application No. 61/084,140 filed Jul. 28, 2008, entitled Metal Oxide-Graphene Hybrid Nanostructures and Method of Making.

The invention was made with Government support under Contract DE-AC0676RLO 1830, awarded by the U.S. Department of Energy. The Government has certain rights in the invention.

## TECHNICAL FIELD

This invention relates to nanocomposite materials of graphene in electrical communication with metal oxides and methods for forming nanocomposite materials of graphene in electrical communication with metal oxides.

## BACKGROUND OF THE INVENTION

Graphene is generally described as a one-atom-thick planar sheet of sp<sup>2</sup>-bonded carbon atoms that are densely packed in a honeycomb crystal lattice. The carbon-carbon bond length in graphene is approximately 0.142 nm. Graphene is the basic structural element of some carbon allotropes including graphite, carbon nanotubes and fullerenes. Graphene exhibits unique properties, such as very high strength and very high conductivity. Those having ordinary skill in the art recognize that many types of materials and devices may be improved if graphene is successfully incorporated into those materials and devices, thereby allowing them to take advantage of graphene's unique properties. Thus, those having ordinary skill in the art recognize the need for new methods of fabricating graphene and composite materials that incorporated graphene.

Graphene has been produced by a variety of techniques. For example, graphene is produced by the chemical reduction of graphene oxide, as shown in Gomez-Navarro, C.; Weitz, R. T.; Bittner, A. M.; Scolari, M.; Mews, A.; Burghard, M.; Kern, K. Electronic Transport Properties of Individual Chemically Reduced Graphene Oxide Sheets. and *Nano Lett.* 2007, 7, 3499-3503. Si, Y.; Samulski, E. T. Synthesis of Water Soluble Graphene. *Nano Lett.* 2008, 8, 1679-1682.

While the resultant product shown in the forgoing methods is generally described as graphene, it is clear from the specific capacity of these materials that complete reduction is not achieved, because the resultant materials do not approach the theoretical specific capacity of neat graphene. Accordingly, at least a portion of the graphene is not reduced, and the resultant material contains at least some graphene oxide. As used herein, the term "graphene" should be understood to encompass materials such as these, that contain both graphene and small amounts of graphene oxide.

For example, functionalized graphene sheets (FGSs) prepared through the thermal expansion of graphite oxide as shown in McAllister, M. J.; LiO, J. L.; Adamson, D. H.; Schniepp, H. C.; Abdala, A. A.; Liu, J.; Herrera-Alonso, M.; Milius, D. L.; CarO, R.; Prud'homme, R. K.; Aksay, I. A. Single Sheet Functionalized Graphene by Oxidation and Thermal Expansion of Graphite. *Chem. Mater.* 2007, 19, 4396-4404 and Schniepp, H. C.; Li, J. L.; McAllister, M. J.; Sai, H.; Herrera-Alonso, M.; Adamson, D. H.; Prud'homme,

2

R. K.; Car, R.; Saville, D. A.; Aksay, I. A. Functionalized Single Graphene Sheets Derived from Splitting Graphite Oxide. *J. Phys. Chem. B* 2006, 110, 8535-8539 have been shown to have tunable C/O ratios ranging from 10 to 500. The term "graphene" as used herein should be understood to include both pure graphene and graphene with small amounts of graphene oxide, as is the case with these materials.

Further, while graphene is generally described as a one-atom-thick planar sheet densely packed in a honeycomb crystal lattice, these one-atom-thick planar sheets are typically produced as part of an amalgamation of materials, often including materials with defects in the crystal lattice. For example, pentagonal and heptagonal cells constitute defects. If an isolated pentagonal cell is present, then the plane warps into a cone shape. Likewise, an isolated heptagon causes the sheet to become saddle-shaped. When producing graphene by known methods, these and other defects are typically present.

The IUPAC compendium of technology states: "previously, descriptions such as graphite layers, carbon layers, or carbon sheets have been used for the term graphene . . . it is not correct to use for a single layer a term which includes the term graphite, which would imply a three-dimensional structure. The term graphene should be used only when the reactions, structural relations or other properties of individual layers are discussed". Accordingly, while it should be understood that while the terms "graphene" and "graphene layer" as used in the present invention refers only to materials that contain at least some individual layers of single layer sheets, the terms "graphene" and "graphene layer" as used herein should therefore be understood to also include materials where these single layer sheets are present as a part of materials that may additionally include graphite layers, carbon layers, and carbon sheets.

The unique electrical and mechanical properties of graphene have led to interest in its use in a variety of applications. For example, electrochemical energy storage has received great attention for potential applications in electric vehicles and renewable energy systems from intermittent wind and solar sources. Currently, Li-ion batteries are being considered as the leading candidates for hybrid, plug-in hybrid and all electrical vehicles, and possibly for utility applications as well. However, many potential electrode materials (e.g., oxide materials) in Li-ion batteries are limited by slow Li-ion diffusion, poor electron transport in electrodes, and increased resistance at the interface of electrode/electrolyte at high charging-discharging rates.

To improve the charge-discharge rate performance of Li-ion batteries, extensive work has focused on improving Li-ion and/or electron transport in electrodes. The use of nanostructures (e.g., nanoscale size or nanoporous structures) has been widely investigated to improve the Li-ion transport in electrodes by shortening Li-ion insertion/extraction pathway. In addition, a variety of approaches have also been developed to increase electron transport in the electrode materials, such as conductive coating (e.g., carbon), and uses of conductive additives (e.g., conductive oxide wires or networks, and conductive polymers). Recently, TiO<sub>2</sub> has been extensively studied to demonstrate the effectiveness of nanostructures and conductive coating in these devices.

TiO<sub>2</sub> is particularly interesting because it is an abundant, low cost, and environmentally benign material. TiO<sub>2</sub> is also structurally stable during Li-insertion/extraction and is intrinsically safe by avoiding Li electrochemical deposition. These properties make TiO<sub>2</sub> particularly attractive for large scale energy storage.

Another way to improve the Li-ion insertion properties is to introduce hybrid nanostructured electrodes that intercon-

nect nanostructured electrode materials with conductive additive nanophases. For example, hybrid nanostructures, e.g.,  $V_2O_5$ —carbon nanotube (CNT) or anatase  $TiO_2$ —CNT hybrids,  $LiFePO_4$ — $RuO_2$  nanocomposite, and anatase  $TiO_2$ — $RuO_2$  nanocomposite, combined with conventional carbon additives (e.g., Super P carbon or acetylene black) have demonstrated an increased Li-ion insertion/extraction capacity in the hybrid electrodes at high charge/discharge rates.

While the hybrids or nanocomposites offer significant advantages, some of the candidate materials to improve the specific capacity, such as  $RuO_2$  and CNTs, are inherently expensive. In addition, conventional carbon additives at high loading content (e.g., 20 wt % or more) are still needed to ensure good electron transport in fabricated electrodes. To improve high-rate performance and reduce cost of the electrochemically active materials, it is important to identify high surface area, inexpensive and highly conductive nanostructured materials that can be integrated with electrochemical active materials at nanoscale.

Those having ordinary skill in the art recognize that graphene may be the ideal conductive additive for applications such as these hybrid nanostructured electrodes because of its high surface area (theoretical value of  $2630\text{ m}^2/\text{g}$ ), which promises improved interfacial contact, the potential for low manufacturing cost as compared to CNTs, and high specific capacity. Recently, high-surface-area graphene sheets were studied for direct Li-ion storage by expanding the layer spacing between the graphene sheets as described in Yoo, E.; Kim, J.; Hosono, E.; Zhou, H.-s.; Kudo, T.; Honma, I. Large Reversible Li Storage of Graphene Nanosheet Families for Use in Rechargeable Lithium Ion Batteries. *Nano Lett.* 2008, 8, 2277-2282. In addition to these studies, graphene has also been used to form composite materials with  $SnO_2$  for improving capacity and cyclic stability of the anode materials as described in Paek, S.-M.; Yoo, E.; Honma, I. Enhanced Cyclic Performance and Lithium Storage Capacity of  $SnO_2$ /Graphene Nanoporous Electrodes with Three-Dimensionally Delaminated Flexible Structure. *Nano Lett.* 2009, 9, 72-75.

While these results were promising, they fell short of producing materials exhibiting specific capacity approaching the theoretical possibilities. For example, while it has been shown that graphene may be combined with certain metal oxides, the graphene materials in these studies fall far short of the theoretical maximum conductivity of single-sheet graphene. Further, those having ordinary skill in the art recognize that the carbon:oxygen ratio and the specific surface area of graphene provide an excellent proxy to measure the relative abundance of high conductivity single-sheets in a given sample. This is because the C:O ratio is a good measure of the degree of "surface functionalization" which affects conductivity, and the surface area conveys the percentage of single-sheet graphene in the synthesized powder.

With respect to battery configurations in the prior art, research has been directed toward long life and low cost. Better performance is demonstrated by minimizing the internal resistance and irreversible heat generation. These properties are shown when degradation is minimized over multiple charge/discharge cycles.

Accordingly, those having ordinary skill in the art recognize that improvements to these methods are required to achieve the potential of using graphene nanostructures in these and other applications. Specifically, those skilled in the art recognize the need for new methods that produce nanocomposite materials of graphene and metal oxides that exhibit greater specific capacity than demonstrated in these prior art methods. Further, those having ordinary skill in the

art recognize the need for improved batteries that provide lower internal resistance and irreversible heat generation as evidenced by minimal degradation over multiple charge/discharge cycles.

The present invention fulfills those needs, and provides such improved composite nanostructures of graphene layers and metal oxides that exhibit specific capacities heretofore unknown in the prior art. The present invention further provides improved and novel methods for forming these composite nanostructures, and improved and novel devices that take advantage of the new and unique properties exhibited by these materials. The present invention meets these objectives by making nanostructures of graphene layers and metal oxides where the C:O ratio of the graphene layers in these nanostructures is between 15-500:1, and preferably 20-500:1, and the surface area of the graphene layers in these nanostructures is  $400\text{--}2630\text{ m}^2/\text{g}$ , and preferably  $600\text{--}2630\text{ m}^2/\text{g}$ , as measured by BET nitrogen adsorption at 77K. While those having ordinary skill in the art have recognized the desirability of having C:O ratios and surface areas this high in the graphene of nanostructures of graphene and metal oxides, the prior art methods have failed to produce them.

The present invention further provides batteries of  $LiFePO_4$  cathode and anatase/graphene composite anodes with better performance than those known in the art, and with minimal internal resistance and irreversible heat generation. The unique Li-ion cells of the present invention have demonstrated negligible degradation after 700 cycles at  $1\text{ C}_m$  rate.

#### SUMMARY OF THE INVENTION

The present invention thus includes a nanocomposite material comprising a metal oxide in electrical communication with at least one graphene layer. The metal oxide is preferably  $M_xO_y$ , and where M is selected from the group consisting of Ti, Sn, Ni, Mn, V, Si, Co and combinations thereof. The nanocomposite materials of the present invention are readily distinguished from the prior art because they exhibit a specific capacity of at least twice that of the metal oxide material without the graphene at a charge/discharge rate greater than about 10 C.

For example, while not meant to be limiting, an example where titania is used as the metal oxide, the resulting nanocomposite material has a specific capacity at least twice that of a titania material without graphene at a charge/discharge rate greater than about 10 C. Continuing the example, where titania is used as the metal oxide, the titania may be provided in a mesoporous form, and the mesoporous titania may further be provided in a rutile crystalline structure, or in an anatase crystalline structure.

The nanocomposite material of the present invention preferably is provided as graphene layers with metal oxides uniformly distributed throughout the nanoarchitecture of the layers. Preferably, but not meant to be limiting, the nanocomposite material of the present invention provides a metal oxide in electrical communication with at least one graphene layer that has a thickness between 0.5 and 50 nm. More preferably, but also not meant to be limiting, the nanocomposite material of the present invention provides a metal oxide in electrical communication with at least one graphene layer that has a thickness between 2 and 10 nm. Preferably, the carbon to oxygen ratio (C:O) of the graphene in the nanostructures of the present invention is between 15-500:1, and more preferably between 20-500:1. Preferably, the surface area of the graphene in the nanostructures of the present invention is between  $400\text{--}2630\text{ m}^2/\text{g}$ , and more preferably between  $600\text{--}2630\text{ m}^2/\text{g}$ , as measured by BET nitrogen adsorption at 77K.

5

Another aspect of the present invention is a method for forming the nanocomposite materials of graphene in electrical communication with metal oxide. One method for forming these materials consists of the steps of providing graphene in a first suspension; dispersing the graphene with a surfactant; adding a metal oxide precursor to the dispersed graphene to form a second suspension; and precipitating the metal oxide from the second suspension onto at least one surface of the dispersed graphene. In this manner, a nanocomposite material of at least one metal oxide in electrical communication with at least one graphene layer is thereby formed. The nanocomposite materials formed in this manner are readily distinguished from materials formed by prior art methods because they exhibit a specific capacity of at least twice that of the metal oxide material without the graphene at a charge/discharge rate greater than about 100.

Preferably, but not meant to be limiting, the first suspension is, at least in part, an aqueous suspension and the surfactant is an anionic surfactant. Also not meant to be limiting, a preferred anionic sulfate surfactant is sodium dodecyl sulfate. The method of the present invention may further comprise the step of heating the second suspension from 50 to 500 degrees C. to condense the metal oxide on the graphene surface. The method of the present invention may also further comprise the step of heating the second suspension from 50 to 500 degrees C. to remove the surfactant.

The present invention also encompasses an energy storage device comprising a nanocomposite material having an active metal oxide compound and one graphene layer arranged in a nanoarchitecture. The energy storage devices of the present invention are readily distinguished from prior art energy storage devices because they exhibit a specific capacity of at least twice that of the metal oxide material without the graphene at a charge/discharge rate greater than about 10 C.

For example, while not meant to be limiting, an example where titania is used as the metal oxide, the energy storage device of the present invention has a specific capacity at least twice that of a titania material without graphene at a charge/discharge rate greater than about 100.

Preferably, but not meant to be limiting, the energy storage device of the present invention is provided as having at least one component having a nanocomposite material having graphene layers with metal oxides uniformly distributed throughout the nanoarchitecture of the layers. Also preferably, but not meant to be limiting, the energy storage device of the present invention is an electrochemical device having an anode, a cathode, an electrolyte, and a current collector, wherein at least one of the anode, cathode, electrolyte, and current collector is fabricated, at least in part, from a nanocomposite material having graphene layers with metal oxides uniformly distributed throughout the nanoarchitecture of the layers.

In embodiments where the energy storage device of the present invention includes a cathode fabricated, at least in part, from a nanocomposite material having graphene layers with metal oxides uniformly distributed throughout the nanoarchitecture of the layers, the graphene in the cathode is preferably, but not meant to be limiting, 5% or less of the total weight of the cathode, and more preferably, but also not meant to be limiting, 2.5% or less of the total weight of the cathode. In this manner, the energy storage devices of the present invention are distinguished from prior art devices which are characterized by having more than 5% of the total weight of the cathode as carbon with no graphene.

In embodiments where the energy storage device of the present invention includes an anode fabricated, at least in part, from a nanocomposite material having graphene layers with

6

metal oxides uniformly distributed throughout the nanoarchitecture of the layers, the graphene in the anode is preferably, but not meant to be limiting, 10% or less of the total weight of anode, and more preferably, but also not meant to be limiting, 5% or less of the total weight of anode. In this manner, the energy storage devices of the present invention are distinguished from prior art devices which are characterized by having more than 10% of the total weight of the anode as carbon with no graphene.

One embodiment where the present invention is an energy storage device is as a lithium ion battery. In this embodiment, the lithium ion battery has at least one electrode with at least one graphene layer in electrical communication with titania to form a nanocomposite material, and the nanocomposite material has a specific capacity at least twice that of a titania material without graphene at a charge/discharge rate greater than about 10 C. The electrode of this lithium ion battery may further have multiple nanocomposite material layers uniformly distributed throughout the electrode.

The present invention further includes a lithium ion battery having an anode comprising at least one graphene layer in electrical communication with titania to form a nanocomposite material, a cathode comprising a lithium olivine structure, and an electrolyte. Preferably, the graphene layer has a carbon to oxygen ratio of between 15 to 1 and 500 to 1 and a surface area of between 400 and 2630 m<sup>2</sup>/g. Preferably, the nanocomposite material has a specific capacity at least twice that of a titania material without graphene material at a charge/discharge rate greater than about 100. Preferably, the olivine structure of the cathode of the lithium ion battery of the present invention is LiMPO<sub>4</sub> where M is selected from the group consisting of Fe, Mn, Co, Ni and combinations thereof.

Preferably, the graphene and titania are sufficiently dispersed in the anode of the lithium ion battery of the present invention such that the specific capacity decays less than 15 percent over 300 charge/discharge cycles.

More preferably, the graphene and titania are sufficiently dispersed in the anode of the lithium ion battery of the present invention such that the specific capacity decays less than 5 percent over 300 charge/discharge cycles.

More preferably, the graphene and titania are sufficiently dispersed in the anode of the lithium ion battery of the present invention such that the specific capacity decays less than 2 percent over 300 charge/discharge cycles.

More preferably, the graphene and titania are sufficiently dispersed in the anode of the lithium ion battery of the present invention such that the specific capacity decays less than 1 percent over 300 charge/discharge cycles.

More preferably, the graphene and titania are sufficiently dispersed in the anode of the lithium ion battery of the present invention such that the specific capacity decays less than 1 percent over 700 charge/discharge cycles.

It is also preferred that the graphene layer of the lithium ion battery of the present invention have a carbon to oxygen ratio of between 15 to 1 and 500 to 1 and a surface area of between 400 and 2630 m<sup>2</sup>/g.

It is also preferred that the nanocomposite material of the lithium ion battery of the present invention have a specific capacity at least twice that of a titania material without graphene material at a charge/discharge rate greater than about 10 C.

#### BRIEF DESCRIPTION OF THE DRAWINGS

The following detailed description of the embodiments of the invention will be more readily understood when taken in conjunction with the following drawing, wherein:

7

FIG. 1 is a schematic illustration of the present invention showing anionic sulfate surfactant mediated stabilization of graphene and growth of  $\text{TiO}_2$ —FGS hybrid nanostructures.

FIG. 2 is a graph showing high energy resolution photo-emission spectra of the C 1s region in functionalized graphene sheets (FGS) used in one embodiment of the present invention.

FIG. 3 are Raman spectra of rutile  $\text{TiO}_2$ —FGS and FGS in one embodiment of the present invention.

FIG. 4(a) is a photograph of FGS (left) and SDS-FGS aqueous dispersions (right); FIG. 4(b) is a graph of the UV-Vis absorbance of the SDS-FGS aqueous dispersion.

FIG. 5 is an XRD pattern of one embodiment of the present invention, an anatase  $\text{TiO}_2$ —FGS and rutile  $\text{TiO}_2$ —FGS hybrid material. Standard diffraction peaks of anatase  $\text{TiO}_2$  (JCPDS No. 21-1272) and rutile  $\text{TiO}_2$  (JCPDS No. 21-1276) are shown as vertical bars.

FIG. 6(a)-(g) are TEM and SEM images of the nanocomposite materials of various embodiments of the present invention at selected magnifications.

FIG. 7(a)-(f) are graphs showing the electrical performance of one embodiment of the present invention. FIG. 7(a) shows the voltage profiles for control rutile  $\text{TiO}_2$  and rutile  $\text{TiO}_2$ —FGS (0.5 wt % FGS) hybrid nanostructures at C/5 charge-discharge rates. FIG. 7(b) shows the specific capacity of control rutile  $\text{TiO}_2$  and the rutile  $\text{TiO}_2$ —FGS hybrids at different charge/discharge rates; FIG. 7(c) shows the cycling performance of the rutile  $\text{TiO}_2$ —FGS up to 100 cycles at 1 C charge/discharge rates after testing at various rates shown in FIG. 7(b). FIG. 7(d) shows the voltage profiles for control anatase  $\text{TiO}_2$  and anatase  $\text{TiO}_2$ —FGS (2.5 wt % FGS) hybrid nanostructures at C/5 charge-discharge rates. FIG. 7(e) shows the specific capacity of control anatase  $\text{TiO}_2$  and the anatase  $\text{TiO}_2$ —FGS hybrids at different charge/discharge rates; FIG. 7(f) shows the cycling performance of the anatase  $\text{TiO}_2$ —FGS up to 100 cycles at 1 C charge/discharge rates after testing at various rates shown in FIG. 7(e).

FIG. 8 is a graph showing a plot of coulombic efficiency versus cycle number of  $\text{TiO}_2$ —FGS hybrids of one embodiment of the present invention at various charge/discharge rate between 1–3 V vs.  $\text{Li/Li}^+$ .

FIG. 9 is a graph showing the capacity of functionalized graphene sheets of one embodiment of the present invention as function of cycling numbers between 1–3 V vs.  $\text{Li/Li}^+$ .

FIG. 10(a) is a graph showing the impedance measurement of coin cells using the electrode materials of control rutile  $\text{TiO}_2$  and rutile  $\text{TiO}_2$ —FGS hybrids with different weight percentage of FGSs. FIG. 10(b) is a graph showing the specific capacity of rutile  $\text{TiO}_2$ —CNT and rutile  $\text{TiO}_2$ —FGS at 30 C rate with different percentages of graphene.

FIG. 11 is a graph showing the specific capacity of control rutile  $\text{TiO}_2$  (10 wt % Super P) and rutile  $\text{TiO}_2$ —FGS hybrids (10 wt % FGS) at different charge/discharge rates. The rutile  $\text{TiO}_2$ —FGS hybrid electrode was prepared by mixing the calcined hybrid with PVDF binder at a mass ratio of 90:10. The control  $\text{TiO}_2$  electrode was prepared by mixing control  $\text{TiO}_2$  powder, Super P and PVDF binder at a mass ratio of 80:10:10.

FIG. 12 is an SEM image of  $\text{TiO}_2$ /FGS hybrid materials made in one embodiment of the present invention without using SDS as a stabilizer. As shown,  $\text{TiO}_2$  and FGS domains are separated from each other with minor  $\text{TiO}_2$  coated on FGS.

FIGS. 13 (a) and (b) are the FESEM image (a) and XRD pattern (b) of a sample of nanostructured  $\text{LiFePO}_4$ .

FIG. 14 are graphs showing the electrochemical cycling at various C rates for (a) anatase  $\text{TiO}_2$ /graphene, (b)  $\text{LiFePO}_4$  (c)

8

$\text{LiFePO}_4$ -anatase  $\text{TiO}_2$ /graphene and voltage profiles of charge/discharge at various C rates for (d) anatase  $\text{TiO}_2$ /graphene, (e)  $\text{LiFePO}_4$  and (f)  $\text{LiFePO}_4$ -anatase  $\text{TiO}_2$ /graphene.

FIG. 15 are graphs showing the performance characteristics of the present invention described in the experiments. FIG. 15 (a) shows the dq/dv peaks, FIG. 15 (b) is Ragone plot comparison of  $\text{LiFePO}_4$ , anatase  $\text{TiO}_2$ /graphene and  $\text{LiFePO}_4$ -anatase  $\text{TiO}_2$ /graphene full-cell and FIG. 15 (c) is a graph showing cycling performance of full cell at 1  $C_m$  rate ( $C_m$ : measured C rate).

#### DETAILED DESCRIPTION OF THE PREFERRED EMBODIMENTS

For the purposes of promoting an understanding of the principles of the invention, reference will now be made to the embodiments illustrated in the drawings and specific language will be used to describe the same. It will nevertheless be understood that no limitations of the inventive scope is thereby intended, as the scope of this invention should be evaluated with reference to the claims appended hereto. Alterations and further modifications in the illustrated devices, and such further applications of the principles of the invention as illustrated herein are contemplated as would normally occur to one skilled in the art to which the invention relates.

A series of experiments were conducted to demonstrate certain embodiments of the present invention. In some of these experiments, anionic sulfate surfactants were used to assist the stabilization of graphene in aqueous solutions and facilitate the self-assembly of in-situ grown nanocrystalline  $\text{TiO}_2$ , rutile and anatase, with graphene. These nanostructured  $\text{TiO}_2$ -graphene hybrid materials were then used for investigation of Li-ion insertion properties. The hybrid materials showed significantly enhanced Li-ion insertion/extraction in  $\text{TiO}_2$ . The specific capacity was more than doubled at high charge rates, as compared with the pure  $\text{TiO}_2$  phase. The improved capacity at high charge-discharge rate may be attributed to increased electrode conductivity in the presence of a percolated graphene network embedded into the metal oxide electrodes. While not to be limiting, these are among the features that distinguish the methods, materials, and devices of the present invention from the prior art.

These experiments thereby demonstrated that the use of graphene as a conductive additive in self-assembled hybrid nanostructures enhances high rate performance of electrochemical active materials. While the metal oxide  $\text{TiO}_2$  was selected as a model electrochemical active oxide material, the method of the present invention is equally applicable to all metal oxides.

This set of experiments utilized a one-step synthesis approach to prepare metal oxide-graphene hybrid nanostructures. In these experiments, the reduced and highly conductive form of graphene is hydrophobic and oxides are hydrophilic. The present invention's use of surfactants not only solved the hydrophobic/hydrophilic incompatibility problem, but also provides a molecular template for controlled nucleation and growth of the nanostructured inorganics, resulting in a uniform coating of the metal oxide on the graphene surfaces.

This approach, schematically illustrated in FIG. 1, starts with the dispersion of the graphene layers with an anionic sulfate surfactant. For example, but not meant to be limiting, sodium dodecyl sulfate. The method then proceeds with the self-assembly of surfactants with the metal oxide precursor and the in-situ precipitation of metal oxide precursors to produce the desired oxide phase and morphology.

In a typical preparation of rutile  $\text{TiO}_2$ —FGS hybrid materials (e.g., 0.5 wt % FGS), 2.4 mg FGSs and 3 mL SDS aqueous solution (0.5 mol/L) were mixed together. The mixture was diluted to 15 mL and sonicated for 10–15 min using a BRANSON SONIFER S-450A, 400 W. 25 mL  $\text{TiCl}_3$  (0.12 mol/L) aqueous solution was then added into as-prepared SDS-FGS dispersions while stirring. Then, 2.5 mL  $\text{H}_2\text{O}_2$  (1 wt %) was added dropwise followed by de-ionized water under vigorous stirring until reaching a total volume of 80 mL. In a similar manner, 0.8, 26.4, and 60 mg FGSs were used to prepare the hybrid materials with 0.17, 5, and 10 wt % FGS, respectively.

Rutile  $\text{TiO}_2$ —CNT (0.5 wt % carbon nanotubes) hybrid materials were also prepared using corresponding single-wall CNTs (2.4 mg) according to the above method.

In a typical preparation of anatase  $\text{TiO}_2$ —FGS hybrid materials (e.g., 2.5 wt % FGS), 13 mg FGS and 0.6 mL SDS aqueous solution (0.5 mol/L) were mixed and sonicated to prepare an SDS-FGS dispersion. 25 mL  $\text{TiCl}_3$  (0.12 mol/L) aqueous solution was added into as-prepared SDS-FGS dispersions while stirring followed by the addition of 5 mL 0.6 M  $\text{Na}_2\text{SO}_4$ . 2.5 mL  $\text{H}_2\text{O}_2$  (1 wt %) was then added dropwise followed by addition of de-ionized water under vigorous stirring until reaching a total volume of 80 mL.

All of these resulting mixtures were further stirred in a sealed polypropylene flask at 90° C. for 16 h. The precipitates were separated by centrifuge followed by washing with de-ionized water and ethanol. The centrifuging and washing processes were repeated 3 times. The product was then dried in a vacuum oven at 70° C. overnight and subsequently calcined in static air at 400° C. for 2 h.

The thermal gravimetric analysis (TGA) indicated approximately 50 wt % percentage loss of FGSs during calcination in air at 400° C. for 2 h. The weight percentage of the graphene in the hybrid materials was thus correspondingly normalized, which is consistent with TGA of the hybrid materials.

The samples were characterized by XRD patterns obtained on a Philips Xpert X-ray diffractometer using  $\text{CuK}_\alpha$  radiation at  $\lambda=1.54$  Å. The TEM imaging was performed on a JEOL JSM-2010 TEM operated at 200 kV. SEM images were obtained on an FEI Helios Nanolab dual-beam focused ion beam/scanning electron microscope (FIB/SEM) operated at 2 kV. XPS characterization was performed using a Physical Electronics Quantum 2000 Scanning ESCA Microprobe with a focused monochromatic  $\text{AlK}_\alpha$  X-ray (1486.7 eV) source and a spherical section analyzer. Electrochemical experiments were performed with coin cells (Type 2335, half-cell) using Li foil as counter electrode. The working electrode was prepared using the mixture of calcined  $\text{TiO}_2$ —FGS or control  $\text{TiO}_2$ , Super P and poly(vinylidene fluoride) (PVDF) binder dispersed in N-methylpyrrolidone (NMP) solution. For the preparation of rutile  $\text{TiO}_2$  electrode (less than 5 wt % graphene), the mass ratio of rutile  $\text{TiO}_2$ -hybrid or control rutile  $\text{TiO}_2$ , Super P and PVDF was 80:10:10. For the preparation of anatase  $\text{TiO}_2$  electrode, the mass ratio was 70:20:10 and 80:10:10 for control anatase  $\text{TiO}_2$  and anatase  $\text{TiO}_2$ —FGS hybrid (2.5 wt % FGS), respectively.

Rutile  $\text{TiO}_2$ —FGS hybrid (10 wt % FGS) electrode was prepared with a mass ratio of hybrid and PVDF binder at 90:10 without Super P. The resultant slurry was then uniformly coated on an aluminum foil current collector and dried overnight in air. The electrolyte used was 1 M  $\text{LiPF}_6$  dissolved in a mixture of ethyl carbonate (EC) and dimethyl carbonate (DMC) with the volume ratio of 1:1. The coin cells were assembled in an argon-filled glove box. The electrochemical performance of  $\text{TiO}_2$ -graphene was characterized with an

Arbin Battery Testing System at room temperature. The electrochemical tests were performed between 3~1 V vs.  $\text{Li}^+/\text{Li}$  and C-rate currents applied were calculated based on a rutile  $\text{TiO}_2$  theoretical capacity of 168 mAh/g.

Functionalized graphene sheets (FGSs) used in this study were prepared through the thermal expansion of graphite oxide according to the method shown in McAllister, M. J.; LiO, J. L.; Adamson, D. H.; Schniepp, H. C.; Abdala, A. A.; Liu, J.; Herrera-Alonso, M.; Milius, D. L.; CarO, R.; Prud'homme, R. K.; Aksay, I. A. Single Sheet Functionalized Graphene by Oxidation and Thermal Expansion of Graphite. *Chem. Mater.* 2007, 19, 4396-4404 and Schniepp, H. C.; Li, J. L.; McAllister, M. J.; Sai, H.; Herrera-Alonso, M.; Adamson, D. H.; Prud'homme, R. K.; Car, R.; Saville, D. A.; Aksay, I. A. Functionalized Single Graphene Sheets Derived from Splitting Graphite Oxide. *J. Phys. Chem. B* 2006, 110, 8535-8539. As discussed previously, in comparison to the graphene produced by the chemical reduction of graphene oxide, graphene prepared by the thermal expansion approach can have tunable C/O ratios ranging from 10 to 500 and thus its conductivity can be tuned to higher values.

FGSs processing starts with chemical oxidation of graphite flakes to increase the c-axis spacing from 0.34 to 0.7 nm. The resultant graphite oxide is then split by a rapid thermal expansion to yield separated graphene sheets. X-ray photoemission spectroscopy (XPS) of FGSs shows a sharp C1s peak indicating good  $\text{sp}^2$  conjugation as shown in FIG. 2. A small shoulder at 286 eV indicates the existence of some C—O bonds corresponding to the epoxy and hydroxyl functional groups on FGSs.

Sodium dodecyl sulfate (SDS)-FGS aqueous dispersions were prepared by ultrasonication. Similar to the colloidal stabilization of CNTs using SDS shown in Bonard, J. M.; Stora, T.; Salvétat, J. P.; Maier, F.; Stockli, T.; Duschl, C.; Forro, L.; deHeer, W. A.; Chatelain, A. Purification and Size-Selection of Carbon Nanotubes. *Adv. Mater.* 1997, 9, 827-831 and Richard, C.; Balavoine, F.; Schultz, P.; Ebbesen, T. W.; Mioskowski, C. Supramolecular Self-Assembly of Lipid Derivatives on Carbon Nanotubes. *Science* 2003, 300, 775-778, the SDS-FGS aqueous dispersions were stable. Only minor sedimentation was observed after a week at room temperature as shown in FIG. 4a.

UV-Vis spectrum of the SDS-FGS dispersion showed an absorption peak at 275 nm with a broad absorption background (FIG. 4b) consistent with that of aqueous stable graphene sheets. Raman spectra of FGS and calcined  $\text{TiO}_2$ —FGS showed similar G and D bands structure of carbon, indicating that the structure of graphene is maintained during the synthesis procedure, as shown in FIG. 3.

A mild, low-temperature (below 100° C.) crystallization process was carried out to form crystalline  $\text{TiO}_2$  with controlled crystalline phase (i.e., rutile and anatase) on the graphene sheets. The low temperature condition was also important in preventing aggregation of graphene sheets at elevated temperatures. Consistent with previous studies, by the low-temperature oxidative hydrolysis and crystallization, rutile  $\text{TiO}_2$ —FGS is obtained with a minor anatase phase. To obtain anatase  $\text{TiO}_2$ —FGS, additional sodium sulfate was added to the solution to promote the formation of the anatase phase. XRD patterns of the  $\text{TiO}_2$ —FGS hybrids shown in FIG. 5 show the formation of nanocrystalline rutile and anatase metal oxides with an estimated crystalline domain size of 6 and 5 nm, respectively.

Typical morphology of FGSs is shown in the transmission electron microscopy (TEM) image of FIG. 6a. The free standing 2D FGSs are not perfectly flat but display intrinsic microscopic roughening and out-of-plane deformations (wrinkles).



More than 80% of the FGSs have been shown to be single sheets by AFM characterization, when they were deposited onto an atomically smooth, highly oriented pyrolytic carbon (HOPG) template. Some regions appeared as multilayers in the TEM images, which may represent the regions that either have not been fully exfoliated or the regions that have restacked together due to capillary and van der Waals forces experienced during the drying process.

FIGS. 6b to 6e show TEM and scanning electron microscopy (SEM) images of as-grown rutile  $\text{TiO}_2$ —FGS hybrid nanostructures. FIGS. 6b and 6c show planar views of FGSs covered with nanostructured  $\text{TiO}_2$ . Both the edge of graphene and the nanostructure of the  $\text{TiO}_2$  are clearly observable in the higher magnification image of FIG. 6c.

The nanostructured  $\text{TiO}_2$  is composed of rod-like rutile nanocrystals organized in parallel interspaced with the SDS surfactants. The SEM image of FIG. 6d shows randomly oriented rod-like nanostructured rutile lying on the FGS. The cross-section TEM image further confirms that the nanostructured rutile mostly lies on the FGS with the rod length parallel to the graphene surface (FIG. 6e). FIGS. 6f and 6g show plane-view TEM images of anatase  $\text{TiO}_2$ —FGS hybrid nanostructures. FGSs underneath are covered with spherical aggregated anatase  $\text{TiO}_2$  nanoparticles. The dark field TEM image (FIG. 6g) further confirms crystalline  $\text{TiO}_2$  nanoparticles (bright regions) with a diameter of 5 nm spreading over the graphene surface.

It is important to note that the SDS surfactant determines the interfacial interactions between graphene and the oxide materials in promoting the formation of  $\text{TiO}_2$ —hybrid nanostructures. When the surfactant molecules are added, they can adsorb onto graphene through the hydrophobic tails making FGSs highly dispersed and interact with the oxide precursor through the hydrophilic head groups. The cooperative interactions between the surfactant, the graphene, and the oxide precursors lead to the homogeneous mixing of the components, in which the hydrophobic graphene most likely resides in the hydrophobic domains of the SDS micelles. As nanocrystalline  $\text{TiO}_2$  formed, as-grown nanoparticles are then coated to the graphene surfaces since sulfate head groups have strong bonding with  $\text{TiO}_2$ . Without the surfactant, some of the surface functional sites (e.g., carboxylate, epoxy, and hydroxyl groups) on FGSs may provide bonding to  $\text{TiO}_2$  nanoparticles. However, only a very small amount of the metal oxides will then be attached to graphene through such interactions due to the low number density of these functional groups on FGSs. Thus, in the control samples without the surfactant, FGSs are barely covered with the metal oxides along with phase separation from  $\text{TiO}_2$  as shown in FIG. 12. This indicates the important role of SDS in the formation of the self-assembled hybrid nanostructures.

To examine the effectiveness of FGSs in improving the rate capability of the electrode, we investigated the Li-ion insertion/extraction properties in the  $\text{TiO}_2$ —FGS hybrid materials. The electrodes were fabricated in a conventional way by mixing the hybrid materials with Super P carbon additive and a PVDF binder and thus tested in Li-ion battery coin cell. The rutile  $\text{TiO}_2$ —FGS hybrid showed a slope profile of voltage-capacity relationship at both the charge and discharge state as shown in FIG. 7a, similar to that of control rutile  $\text{TiO}_2$  and nanostructured rutile studied previously as reported in Hu, Y. S.; Kienle, L.; Guo, Y. G.; Maier, J. High Lithium Electroactivity of Nanometer-Sized Rutile  $\text{TiO}_2$ . *Adv. Mater.* 2006, 18, 1421-1426. As shown in FIG. 7b, with the incorporation of FGSs, the specific capacity of rutile  $\text{TiO}_2$  in the hybrids (0.5 wt % FGS) increased at all charge/discharge rates compared with the control rutile  $\text{TiO}_2$ . The relative increase in specific

capacity is especially larger at higher rates. For instance, at a rate of 30 C (2 min of charging or discharging), the specific capacity of the rutile  $\text{TiO}_2$ —FGS hybrid material is 87 mAh/g which is more than double the high rate capacity (35 mAh/g) of the control rutile  $\text{TiO}_2$  as shown in FIG. 7b.

The voltage-capacity profile of anatase  $\text{TiO}_2$ —FGS (2.5 wt % FGS) at C/5 rate shows plateaus around 1.8 V (discharge process) and 1.9 V (charge process) is shown in FIG. 7d, which is similar to that of control anatase  $\text{TiO}_2$  and nanostructured anatase. The plateaus are related to the phase transition between the tetragonal and orthorhombic phases with Li insertion into anatase  $\text{TiO}_2$ . Similar to rutile  $\text{TiO}_2$ —FGS, the specific capacity of the anatase  $\text{TiO}_2$ —FGS hybrid is enhanced at all charge-discharge rates as shown in FIG. 7e. The specific capacity of the anatase  $\text{TiO}_2$ —FGS at the rate of 30 C is as high as 96 mAh/g compared with 25 mAh/g of control anatase  $\text{TiO}_2$ . Furthermore, the coulombic efficiencies of  $\text{TiO}_2$ —FGS hybrids at various charge/discharge rates are greater than 98% as shown in FIG. 8. Both rutile and anatase  $\text{TiO}_2$ —FGS hybrids show good capacity retention of the Li-ion insertion/extraction with over 90% capacity retention after 100 cycles at a 1 C rate, as shown in FIGS. 7c and 7f.

To identify the capacity contribution from FGSs, the Li-ion insertion/extraction behavior of the FGSs was also studied. The initial capacity of FGS of 100 mAh/g with 50% irreversible loss is observed between 1-3 V potential window applied, which is consistent with a recent study of Li-ion storage in graphene described in Yoo, E.; Kim, J.; Hosono, E.; Zhou, H.-s.; Kudo, T.; Honma, I. Large Reversible Li Storage of Graphene Nanosheet Families for Use in Rechargeable Lithium Ion Batteries. *Nano Lett.* 2008, 8, 2277-2282. However, the specific capacity of FGS rapidly decreases to 25 mAh/g within 10 cycles. At higher charge/discharge rates, FGS has almost negligible Li-ion insertion as shown in FIG. 9. For 1 wt % FGS hybrids, the capacity contribution from FGS itself after 2 cycles can be a maximum value of 0.4 mAh/g. Thus, the increase of the specific capacity at high rate is not attributed to the capacity of the graphene additive itself in the hybrid materials.

To further understand the improved high-rate performance, electrochemical impedance spectroscopy measurements on rutile  $\text{TiO}_2$ —FGS hybrid materials were performed after cycles. The Nyquist plots of the rutile  $\text{TiO}_2$ —FGS electrode materials with different percentage of graphene cycled in electrolyte, as shown in FIG. 10(a), all show depressed semicircles at high frequencies. As electrolyte and electrode fabrication are similar between each electrode, the high frequency semicircle should relate to the internal resistance of the electrode. We estimate that the resistivity of the cells decreased from 93  $\Omega$  for the pure  $\text{TiO}_2$  to 73  $\Omega$  with the addition of only 0.5 wt % graphene.

By increasing the graphene percentage in the hybrid materials further, the specific capacity is slightly increased, e.g., to 93 mAh/g in the hybrid material with 5 wt % FGS, indicating that a kinetic capacity limitation may be reached by only improving the electrode conductivity with the incorporation of FGSs as shown in FIG. 10(b). Rutile  $\text{TiO}_2$ —CNT hybrids prepared and tested under similar conditions showed poorer performance at identical carbon loadings than the rutile  $\text{TiO}_2$ —FGS hybrid anodes, as shown in the yellow bar in FIG. 10(b). Similarly, hybrid nanostructures prepared using solution reduced graphene oxides also showed even poorer performance, indicating the importance of the highly conductive graphene phase of FGSs.

To study the properties of electrode materials without any Super P carbon, Li-ion insertion/extraction properties of the rutile  $\text{TiO}_2$ —FGS (10 wt % graphene) were compared with

control rutile  $\text{TiO}_2$  with 10 wt % Super P at high charge-discharge rates. The hybrid material showed a much higher capacity at all charge-discharge rate, as shown in FIG. 11. This result indeed confirms that the graphene in the self-assembled hybrid materials is more effective than the commonly used Super P carbon materials in improving high rate performance of the electrode materials.

The high rate performance is important for applications where fast charge and discharge is needed, such as in load leveling utility applications. The simple self-assembly approach, and the potential low manufacturing cost of graphene of the present invention, thus provide a new pathway for large scale applications of novel hybrid nanocomposite materials for energy storage.

A further set of experiments were conducted to examine Li-ion batteries made with  $\text{LiFePO}_4$  cathode and anatase  $\text{TiO}_2$  based anodes. In these experiments, for cathode,  $\text{LiFePO}_4$  was selected because of its stability, low cost and environmentally friendliness. While having a lower voltage vs. Li of 3.45V, than many other cathode compositions,  $\text{LiFePO}_4$  has been shown to exhibit flat discharge/charge curves during two-phase Li extraction/insertion process and excellent cycling stability due to its unique ordered olivine structure. Similarly, titanium oxide based materials including  $\text{TiO}_2$ -polymorphs and  $\text{Li}_4\text{Ti}_5\text{O}_{12}$  have been shown to exhibit a relative high voltage vs. Li (1~2V), but have open structures that allow Li-insertion/extraction without much structural straining, thus potentially a long cycle life. In addition, the relative high voltage vs. Li of the  $\text{TiO}_2$ -base anodes helps to avoid SEI layer formation, making the battery much safer than the graphite anodes used commercially. Previously, spinel  $\text{Li}_4\text{Ti}_5\text{O}_{12}$  and  $\text{TiO}_2$  (B) have been used as stable anode. However, the anode materials require additional step to synthesize starting from  $\text{TiO}_2$  materials.

Direct use of  $\text{TiO}_2$  would be a low-cost and efficient way to make full cell battery for stationary energy storage. One of disadvantage of  $\text{TiO}_2$  includes low conductivity and therefore slow electrochemical kinetics. In this study, a full cell Li-ion battery using  $\text{LiFePO}_4$  cathode and anatase  $\text{TiO}_2$ /graphene anode were demonstrated. The  $\text{LiFePO}_4$ -anatase  $\text{TiO}_2$ /graphene cells were evaluated for electrochemical performance.

Fine structured  $\text{LiFePO}_4$  was synthesized using  $\text{LiCOOCH}_3 \cdot 2\text{H}_2\text{O}$  (reagent grade, procured from Sigma),  $\text{FeC}_2\text{O}_4 \cdot 2\text{H}_2\text{O}$  (99%, procured from Aldrich),  $\text{NH}_4\text{H}_2\text{PO}_4$  (99.999%, procured from Sigma-Aldrich), oleic acid (FCC, FG, procured from Aldrich) and paraffin wax (ASTM D 87, mp. 53~57° C., procured from Aldrich).  $\text{NH}_4\text{H}_2\text{PO}_4$  was milled with oleic acid for 1 h using high energy mechanical mill (HEMM, SPEX 8000M) in a stainless steel vial and balls. After paraffin wax was added and milled for 30 min, iron oxalate was added and milled for 10 min. Finally, Li acetate was added and milled for 10 min. The overall molar ratio is Li:Fe:P:Oleic acid=1:1:1:1 with paraffin addition twice the weight of oleic acid. The precursor paste was dried in oven at 110° C. for 30 min followed by heat-treatment in tube furnace at 500° C. for 8 h under UHP-3%  $\text{H}_2$ /97% Ar gas flow with ramping rate of 5° C./min.

After  $\text{LiFePO}_4$  was synthesized, 10% carbon black by weight was added and milled in planetary mill for 4 h (Retsch 100CM) at 400 rpm. Anatase  $\text{TiO}_2$ /graphene composite (2.5 wt % Graphene) was obtained by self assembly approach described herein. X-ray diffraction (XRD) pattern (Philips Xpert) was obtained using  $\text{CuK}\alpha$  (1.54 Å) radiation. Microstructure of  $\text{LiFePO}_4$  was analyzed by a field-emission scanning electron microscope (FESEM, FEI Nova 600).

For electrochemical evaluations, the cathode and anode comprised of active material, Super P and poly(vinylidene fluoride) (PVDF) binder were dispersed in N-methylpyrrolidone (NMP) solution in a weight ratio of 80:10:10 for the anatase  $\text{TiO}_2$ /graphene anode and 90:3:7 for  $\text{LiFePO}_4$ /C cathode, respectively. Both cathode and anode slurries were then coated on an Al foil. The performance of  $\text{LiFePO}_4$  and anatase  $\text{TiO}_2$ /graphene electrodes were evaluated, both in half and full 2325 coin cells (National Research Council, Canada) at room temperature in 1M  $\text{LiPF}_6$  in EC/DMC (2:1) (ethyl carbonate/dimethyl carbonate) electrolyte, using an Arbin Battery Tester (Model BT-2000, Arbin Instruments, College Station, Tex.).

The half-cells using Li as anode were tested between 4.3V and 2V for  $\text{LiFePO}_4$  and 3V to 1V for anatase  $\text{TiO}_2$ /graphene at various C-rate currents based on the theoretical capacity of 170 mAh/g for both cathode and anode. Due to the initial irreversible loss observed for anatase  $\text{TiO}_2$ /graphene anode,  $\text{LiFePO}_4$  loading was ~3 mg/cm<sup>2</sup> and ~1 mg/cm<sup>2</sup> for anatase  $\text{TiO}_2$ /graphene in full cells and tested between 2.5V and 1V where energy and power density was calculated based on the anode weight which is the limiting electrode.

Additional experiments were also conducted to demonstrate alternate paths for fabricating  $\text{TiO}_2$ /graphene anodes. In the first of these experiments, titania/graphene composites (aqueous based, 90 and 72 wt % P-25) were fabricated. In the first of these experiments, an aqueous method using a film type application was shown for forming titania/graphene composites of 90/10 wt % and 72/28 wt % (P-25). To prepare the 90:10 (wt %) titania:graphene suspensions, 23 mg graphene (Vorbek Materials LLC) was dispersed in 50 ml  $\text{H}_2\text{O}$  using 2.3 mg (10 wt %) CTAB (cetyl trimethylammonium bromide) surfactant and ultrasonicated for 15 minutes. For the 72:28 (wt %) titania:graphene suspensions, 77.8 mg of graphene (Vorbek Materials LLC) was dispersed in 50 ml  $\text{H}_2\text{O}$  using 7.78 mg CTAB (cetyl trimethylammonium bromide) surfactant and ultrasonicated for 15 minutes. In a second container, 200 mg nanosized titania powder (Degussa P25) was dispersed in 50 ml  $\text{H}_2\text{O}$  by stirring and ultrasonic mixing for 10 minutes then slowly added to the graphene suspension. The final suspension was then mixed for an additional 4 hours. After mixing, the titania:graphene suspension was filtered, air dried then calcined at 400° C. in a  $\text{H}_2$ /Ar atmosphere for 3 hours.

To prepare the test electrodes, 0.5 ml of poly(vinylidene fluoride) (PVDF) binder dispersed in N-methylpyrrolidone (NMP) solution (0.5 g/20 ml) was added to 0.1125 g of the composite powder and homogenized for 10 minutes. The final slurry was then coated on an Al current collector using a roll applicator (~60 micron). Slurry rheology was adjusted using NMP content and viscosities in the range of approximately 1000-5000 cps produced good quality films. After drying on a hot plate for 5 minutes, circular test electrodes were made using a 1/16" punch. The half-cells (2325 coin cell, National Research Council, Canada) with polypropylene membrane separator (Celgard, Inc.), Li metal anode and reference in 1M  $\text{LiPF}_6$  in EC/DMC (1:1 v/v) (ethyl carbonate/dimethyl carbonate) electrolyte were assembled in a glove box (Mbrazn, Inc.) filled with ultra highly purity (UHP) argon. The electrochemical performance of the  $\text{TiO}_2$ /graphene anode was evaluated using an Arbin Battery Tester BT-2000 (Arbin Inst., College Station, Tex.) at room temperature. The half-cell was tested between 3V and 1V vs. Li at various C rate current based on a theoretical capacity of 168 mAh/g (i.e., 1 C=168 mAh·g<sup>-1</sup>) for anatase.

In the next set of these experiments, an aqueous method using a tape application was shown for forming titania/graphene composites of 90/10 wt % and 72/28 wt % (P-25).

To prepare the 90:10 (wt %) titania:graphene suspensions, 23 mg graphene (Vorbeck Materials LLC) was dispersed in 50 ml H<sub>2</sub>O using 2.3 mg (10 wt %) CTAB (cetyl trimethylammonium bromide) surfactant and ultrasonicated for 15 minutes. For the 72:28 (wt %) titania:graphene suspensions, 77.8 mg of graphene (Vorbeck Materials LLC) was dispersed in 50 ml H<sub>2</sub>O using 7.78 mg CTAB (cetyl trimethylammonium bromide) surfactant and ultrasonicated for 15 minutes. In a second container, 200 mg nanosized titania powder (Degussa P25) was dispersed in 50 ml H<sub>2</sub>O by stirring and ultrasonic mixing for 10 minutes then slowly added to the graphene suspension. The final suspension was then mixed for an additional 4 hours. After mixing, the titania:graphene suspension was filtered, air dried then calcined at 400° C. in a H<sub>2</sub>/Ar atmosphere for 3 hours.

For the preparation of P-25/graphene tapes (90 wt % P-25), 222.2 mg of graphene was dispersed in 250 mL H<sub>2</sub>O using 23 mg of CTAB surfactant and sonicated for 15 min. In a separate container, 2.0 g P-25 was dispersed in 100 mL water by sonication (10 min). The P-25 suspension was slowly added to the graphene dispersion upon stirring and stirred for 4 h. The slurry was filtered, air-dried, and calcined at 400° C. in a H<sub>2</sub>/Ar for 3 h.

To prepare P-25/graphene composite tapes, the calcined powder was first dispersed in water and 7 wt % of PTFE suspension (65 wt % in water, Aldrich) was added upon stirring. After 3 additional hours stirring, the mixture was filtered and dried at 90° C. for 30 min. The powder/PTFE green body was then calendared to the desired thickness (~1-100 microns) using a three-roll mill.

Circular test electrodes were made using a 1/16" punch and dried overnight at 110° C. in a vacuum oven. The half-cells (2325 coin cell, National Research Council, Canada) with polypropylene membrane separator (Celgard, Inc.), Li metal anode and reference in 1M LiPF<sub>6</sub> in EC/DMC (1:1 v/v) (ethyl carbonate/dimethyl carbonate) electrolyte were assembled in a glove box (Mbraun, Inc.) filled with ultra highly purity (UHP) argon. The electrochemical performance of the TiO<sub>2</sub>/graphene anode was then evaluated using an Arbin Battery Tester BT-2000 (Arbin Inst., College Station, Tex.) at room temperature. The half-cell was tested between 3V and 1V vs. Li at various C rate current based on a theoretical capacity of 168 mAh/g (i.e., 1 C=168 mAh·g<sup>-1</sup>) for anatase.

In the next set of these experiments, a non-aqueous method also using a tape application was shown for forming titania/graphene composites of 90/10 wt % and 72/28 wt % (P-25). Nanosized titania powder (Degussa P25) and graphene (Vorbeck Materials LLC) were dispersed in NMP using ultrasonic mixing (30 min) in 90:10 and 72:28 wt % ratios. Total solids loadings between approximately 3-12 wt % were typically useful in preparing the initial suspensions. To these slurries 10 wt % (relative to the solids content) of PVDF binder was added and the mixture stirred 5-16 hours and homogenized if needed. Slurry rheology was adjusted using NMP and viscosities in the range of approximately 1000-5000 cps to produce good quality films.

The final slurry was then coated on an Al current collector using a roll applicator (~60 micron). After drying on a hot plate for 5 minutes, circular test electrodes were made using a 1/16" punch. The half-cells (2325 coin cell, National Research Council, Canada) with polypropylene membrane separator (Celgard, Inc.), Li metal anode and reference in 1M LiPF<sub>6</sub> in EC/DMC (1:1 v/v) (ethyl carbonate/dimethyl carbonate) electrolyte were assembled in a glove box (Mbraun,

Inc.) filled with ultra highly purity (UHP) argon. The electrochemical performance of the TiO<sub>2</sub>/graphene anode was evaluated using an Arbin Battery Tester BT-2000 (Arbin Inst., College Station, Tex.) at room temperature. The half-cell was tested between 3V and 1V vs. Li at various C rate current based on a theoretical capacity of 168 mAh/g (i.e., 1 C=168 mAh·g<sup>-1</sup>) for anatase.

LiFePO<sub>4</sub> was synthesized using molten surfactant approach shown in FIG. 13 where nano-sized LiFePO<sub>4</sub> has been synthesized during the heat-treatment mimicking micelle or hydrothermal approach but with well crystallized particles. The X-ray diffraction analysis (FIG. 13) of LiFePO<sub>4</sub> shows lattice parameters of a=10.329 Å, b=6.005 Å, c=4.691 Å (R<sub>p</sub>: 2.31, R<sub>wp</sub>: 3.06, R<sub>exp</sub>: 2.93) obtained via Rietveld refinement that matched closely to the ideally crystallized LiFePO<sub>4</sub> (JCPDS 81-1173, Pnma(62), a=10.33 Å, b=6.010 Å, c=4.692 Å). The crystallite size was determined to be ~50 nm from the X-ray analysis; primary particle size ranges from 100 to 200 nm from FESEM observation. Anatase TiO<sub>2</sub>/graphene composite show anatase TiO<sub>2</sub> nanoparticles (<20 nm) coated on graphene sheets.

The synthesized anatase TiO<sub>2</sub>/graphene, LiFePO<sub>4</sub> and full-cell configuration have been tested at various C-rates as shown in FIG. 14 (a-e). As shown in FIGS. 14 a. and d., anatase TiO<sub>2</sub>/graphene electrodes demonstrates flat voltage curves at 1.84 V, indicating a classical two-phase electrochemical reaction process of the Li-insertion/extraction. Diffusion of Li ions in anatase TiO<sub>2</sub> framework is known to accompany symmetry transformations between I4<sub>1</sub>/amd and orthorhombic Pmn2<sub>1</sub> when x=0.5 (Li<sub>x</sub>TiO<sub>2</sub>), resulting in a net increase of ~4 vol % of the unit cell leading to capacity fade. Hence, for bulk anatase TiO<sub>2</sub>, x=0.5 is often considered as the maximum electrochemical insertion of Li. However, the reduction in particle size into the nano-regime (<100 nm) alternates the two phase equilibrium phenomenon in the bulk to more of solid solution like Li uptake at the surface thus leading to increased capacity over 0.5 Li per unit formula. As shown in FIG. 14 (a), nano-sized anatase TiO<sub>2</sub>/graphene composite gives more than 175 mAh/g (>0.5 Li) at C/5 rate and demonstrates good cycling capability. The anatase TiO<sub>2</sub>/graphene also exhibited much higher rate response than that of LiFePO<sub>4</sub>, reaching 90 mAh/g at 30 C (equivalent of measured 60 C<sub>m</sub> rate). The LiFePO<sub>4</sub> electrode is characterized by a flat potential at around 3.45 V vs. Li from two-phase Li-extraction/insertion with specific capacity of 110 mAh/g and 71 mAh/g at 5 C and 10 C (equivalent 8 C<sub>m</sub> and 24 C<sub>m</sub>-rate), respectively. The rate capacity of the full cell (FIG. 14(c)) is lower than both cathode and anode half cells due to the lower electronic and ionic conductivity of both cathode and anode compared to Li metal used in half cells. Based on capacity limiting electrode, anatase TiO<sub>2</sub>/graphene, the LiFePO<sub>4</sub>-anatase TiO<sub>2</sub>/graphene full cell delivered ~120 mAh/g at C/2 rate based on anode weight.

Enhancing rate performance is vital not only for achieving higher power but also for minimizing polarization from internal resistance where the latter lead to exothermic irreversible heat generation  $Q_{irr} = I\eta + I^2R_t$  (I: current,  $\eta$ : absolute value of electrode polarization, R: Ohmic resistance, t: time) which plays critical role in heat management required for scaled up systems. Such heat control can extend the cycle life of Li-ion battery.

FIG. 15 (a) shows dq/dv peaks of all electrodes tested at C/5 rate where full cell potential of 1.6V matches the voltage difference between cathode and anode peaks. Ragone plot of all three cells based on active material weight are compared in FIG. 15 (b), the energy density of the full cell is limited by the anatase TiO<sub>2</sub>/graphene due to the same specific capacity but

17

lower voltage compared to  $\text{LiFePO}_4$  whereas the power density is limited by the  $\text{LiFePO}_4$  cathode. The full cell power density of 4.5 kW/kg and energy density of 263 Wh/kg based on capacity limiting anatase  $\text{TiO}_2$ /graphene anode weight lies within these two limitations with  $\text{LiFePO}_4$  cathode limiting the rate, which is opposite to conventional Li-ion batteries using graphite anode.

The cycling performance of the full cell battery at 1  $C_m$  rate shown in FIG. 15 (c) indicates almost no fade even after 700 cycles with coulombic efficiency reaching 100% over the entire cycling test except for the initial few cycles where irreversible loss has been observed. Such a stable full cell cycling performance is unknown in the prior art. The results confirm the ideal reversibility of the lithium ion batteries based on a combination of  $\text{LiFePO}_4$ -anatase  $\text{TiO}_2$ /graphene and the absence of losses due to parasitic processes, such as the electrolyte decomposition.

With emphasis on long life and low cost, along with safety, for the stationary applications, batteries of  $\text{LiFePO}_4$  cathode and anatase/graphene composite anode have been optimized individually to better performance by minimizing the internal resistance and irreversible heat generation. While with relative low energy density, the unique Li-ion cells made from the optimized electrodes demonstrated negligible degradation after 700 cycles at 1  $C_m$  rate. The excellent cycling performance makes the Li-ion battery of the present invention a particularly excellent storage technology for stationary energy storage or in particular in community storage (<100 KWhs).

While the invention has been illustrated and described in detail in the drawings and foregoing description, the same is to be considered as illustrative and not restrictive in character. Only certain embodiments have been shown and described, and all changes, equivalents, and modifications that come within the spirit of the invention described herein are desired to be protected. Any experiments, experimental examples, or experimental results provided herein are intended to be illustrative of the present invention and should not be considered limiting or restrictive with regard to the invention scope. Further, any theory, mechanism of operation, proof, or finding stated herein is meant to further enhance understanding of the present invention and is not intended to limit the present invention in any way to such theory, mechanism of operation, proof, or finding.

Thus, the specifics of this description and the attached drawings should not be interpreted to limit the scope of this invention to the specifics thereof. Rather, the scope of this invention should be evaluated with reference to the claims appended hereto. In reading the claims it is intended that when words such as "a", "an", "at least one", and "at least a portion" are used there is no intention to limit the claims to only one item unless specifically stated to the contrary in the claims. Further, when the language "at least a portion" and/or "a portion" is used, the claims may include a portion and/or the entire items unless specifically stated to the contrary. Likewise, where the term "input" or "output" is used in connection with an electric device or fluid processing unit, it should be understood to comprehend singular or plural and one or more signal channels or fluid lines as appropriate in the

18

context. Finally, all publications, patents, and patent applications cited in this specification are herein incorporated by reference to the extent not inconsistent with the present disclosure as if each were specifically and individually indicated to be incorporated by reference and set forth in its entirety herein.

The invention claimed is:

1. A lithium ion battery having an anode comprising at least one graphene layer having a thickness of 0.5 to 50 nm in contact with titania to form a nanocomposite material, a cathode comprising a lithium olivine structure, and an electrolyte, wherein the nanocomposite material has a specific capacity at least twice that of a titania material without graphene material at a charge/discharge rate greater than 20 C.

2. The lithium ion battery of claim 1 wherein the olivine structure is  $\text{LiMPO}_4$  and M is selected from the group consisting of Fe, Mn, Co, Ni and combinations thereof.

3. A lithium ion battery having an anode comprising at least one graphene layer having a thickness of 0.5 to 50 nm in contact with titania to form a nanocomposite material, a cathode comprising a lithium olivine structure, and an electrolyte wherein the graphene and titania is sufficiently dispersed such that the specific capacity decays less than 5 percent over 300 cycles.

4. A lithium ion battery having an anode comprising at least one graphene layer having a thickness of 0.5 to 50 nm in contact with titania to form a nanocomposite material, a cathode comprising a lithium olivine structure, and an electrolyte wherein the graphene and titania is sufficiently dispersed such that the specific capacity decays less than 2 percent over 300 cycles.

5. A lithium ion battery having an anode comprising at least one graphene layer having a thickness of 0.5 to 50 nm in contact with titania to form a nanocomposite material, a cathode comprising a lithium olivine structure, and an electrolyte wherein the graphene and titania is sufficiently dispersed such that the specific capacity decays less than 1 percent over 300 cycles.

6. A lithium ion battery having an anode comprising at least one graphene layer having a thickness of 0.5 to 50 nm in contact with titania to form a nanocomposite material, a cathode comprising a lithium olivine structure, and an electrolyte wherein the graphene and titania is sufficiently dispersed such that the specific capacity decays less than 1 percent over 700 cycles.

7. A lithium ion battery having an anode comprising at least one graphene layer having a thickness of 0.5 to 50 nm in contact with titania to form a nanocomposite material, a cathode comprising a lithium olivine structure, and an electrolyte wherein the graphene and titania is sufficiently dispersed such that the specific capacity decays less than 15 percent over 300 cycles wherein the nanocomposite material has a specific capacity at least twice that of a titania material without graphene material at a charge/discharge rate greater than 20 C about 10 C.

8. The lithium ion battery of claim 7 wherein the olivine structure is  $\text{LiMPO}_4$  and M is selected from the group consisting of Fe, Mn, Co, Ni and combinations thereof.

\* \* \* \* \*